Cooperative Research Centre for Landscape Environments and Mineral Exploration

MINERAL RESOURCES NEW SOUTH WALES

OPEN FILE REPORT SERIES

REGOLITH ARCHITECTURE AND GEOCHEMISTRY OF THE HERMIDALE AREA OF THE GIRILAMBONE REGION, NORTH-WESTERN LACHLAN FOLD BELT, NSW.

A joint project between CRC LEME and NSW DMR

R.A. Chan, R.S.B. Greene, M. Hicks, B.E.R. Maly,
K.G. McQueen and K.M. Scott

CRC LEME OPEN FILE REPORT 149

March 2003

(CRC for Landscape Environments and Mineral Exploration Report 179 /
NSW DMR Report GS2003/131, 2002.
Second impression 2003)

REGOLITH ARCHITECTURE AND GEOCHEMISTRY OF THE HERMIDALE AREA OF THE GIRILAMBONE REGION, NORTH-WESTERN LACHLAN FOLD BELT, NSW.

A joint project between CRC LEME and NSW DMR

R.A. Chan, R.S.B. Greene, M. Hicks, B.E.R. Maly,
K.G. McQueen and K.M. Scott

CRC LEME OPEN FILE REPORT 149

March 2003

(CRC for Landscape Environments and Mineral Exploration Report 179 /
NSW DMR Report GS2003/131, 2002.
Second impression 2003)

CRC LEME is an unincorporated joint venture between CSIRO-Exploration & Mining, and Land & Water, The Australian National University, Curtin University of Technology, University of Adelaide, Geoscience Australia, Primary Industries and Resources SA, NSW Department of Mineral Resources and Minerals Council of Australia.

Headquarters: CRC LEME c/o CSIRO Exploration and Mining, PO Box 1130, Bentley WA 6102, Australia

The Girilambone (Cobar-Bourke) Project is providing a new knowledge base and developing methodologies for improved mineral exploration in areas of regolith cover in central western NSW. This integrated project has a multidisciplinary team with skills in regolith geology, geomorphology, bedrock geology, geochemistry, geophysics and soil science, working to understand the processes and controls on element dispersion in a variable regolith terrain. This report forms part of a planned series of three reports on work in progress.

Copies of this publication can be obtained from:
The Publications Officer, c/- CRC LEME, CSIRO Exploration and Mining, PO Box 1130, Bentley, WA 6102, Australia. Information on other publications in this series may be obtained from the above, or from http://crcleme.org.au/
Cataloguing-in-publication:
Chan, Roslyn A. et al
Regolith architecture and geochemistry of the Hermidale area of the Girilambone region, North-Western Lachlan foldbelt, NSW.
ISBN 0 643 06847 3
1. Regolith – New South Wales
2. Geochemistry – New South Wales
3. Landforms – New South Wales
I. Chan, R.A.
II. Title
CRC LEME Open File Report 149.
ISSN 1329-4768

Addresses and affiliations of authors

R.A. Chan
Cooperative Research Centre for Landscape Environments and Mineral Exploration
c/- Geoscience Australia
Division of Minerals and Geohazards
GPO Box 378, Canberra 2601
Australian Capital Territory

R.S.B. Greene
Cooperative Research Centre for Landscape Environments and Mineral Exploration
c/- Australian National University
School of Resource and Environmental Management
Department of Geography
PO Box 4, Canberra 0200
Australian Capital Territory

M. Hicks
Cooperative Research Centre for Landscape Environments and Mineral Exploration
c/- NSW Department of Mineral Resources
Geological Survey of New South Wales
Level 5, 29-57 Christie Street
St Leonards, Sydney 2065
New South Wales

B.E.R. Maly
Cooperative Research Centre for Landscape Environments and Mineral Exploration
c/- University of Canberra
Faculty of Applied Science
Division of Science and Design
Canberra 2601
Australian Capital Territory

K.G. McQueen
Cooperative Research Centre for Landscape Environments and Mineral Exploration
c/- University of Canberra
Division of Science and Design
Canberra 2601
Australian Capital Territory

K.M. Scott
Cooperative Research Centre for Landscape Environments and Mineral Exploration
c/- Commonwealth Scientific and Industrial Research Organisation
Division of Exploration and Mining
P.O. Box 136, North Ryde, Sydney 1670
New South Wales

Abstract

Stage 2 of the Girilambone (Cobar-Bourke) Project has involved collaborative work between CRC LEME and the NSW Department of Mineral Resources in the Hermidale area. This work has provided 2275 m of drilling (49 holes, generally 2-4 km apart, along 5 road traverses) for regolith study.

Regolith-landform mapping conducted in association with drill hole logging reveals that colluvial and alluvial sediments cover most of the Hermidale area. Colluvial regolith-landform units are widespread on plains, as well as in areas of higher elevation and relief in the central-south and western parts of the area. Alluvial regolith-landform units are dominant on plains in the central-north and eastern parts. There are also numerous palaeochannels, many of which are defined on 1.5 Vertical Derivative magnetic imagery. However, drilling and mapping indicate that palaeosediments are more extensive than the obvious extent of magnetic sediments. The variable thickness of sediments, both in palaeovalleys within the erosional domain in the west and beneath depositional plains in the east, indicates a palaeo-relief significantly greater than the present relief.

Logging of regolith units through palaeovalley sediments indicates a change in composition from brown to grey clays. This could reflect a change in depositional environment in the palaeovalleys or weathering associated with a palaeo-redox front from higher palaeo-water tables. More detailed facies interpretation is required to resolve these possibilities. The present water table typically ranges from 30-67 m depth and intersects the saprolite well below the base of transported regolith and sediments. Palynology indicates that reduced sediments in the palaeochannel deposits are most likely Late Miocene to Early Pliocene in age.

Dominant bedrock lithologies are phyllite/siltstone, sandy phyllite and sandstone, which are mostly highly weathered to at least 80 m depth. Less weathered felsic volcanic lithologies occur in the southwestern portion of the area. Some mafic and ultramafic bedrock units have also been detected. Regolith carbonates are common throughout the area and are associated with the transported/saprolite or bedrock interface or with sediments higher in the profile.

Mineralogical and geochemical studies of the regolith profiles indicate different mineral assemblages within transported and *in situ* regolith. The transported regolith shows assemblages with kaolinite±illite±smectite, whereas the *in situ* saprolite contains kaolinite±muscovite/phengite ±illite±smectite mineral assemblages.

The change in drilling procedure (*i.e.* purging the vacuum chamber by drilling 2 m of local material and discarding before re-starting drilling at a particular site) has avoided the cross-hole contamination seen during the earlier Sussex phase of drilling. Some caution is advised when interpreting geochemical results for some elements analysed using multi-acid dissolution methods, (*e.g.,* high Cr identifies mafic dykes but the absence of Cr does not preclude material from being mafic). Specifically, Ba, Cr, Ti and Zr values determined by ICP analysis should be regarded as minimum values because of the possibility of incomplete dissolution. Similarly, K and Rb contents may also be low relative to XRF-determined values.

Many near-surface samples show elevated Au, together with Ca, Mg and in some cases Ba-Sr, and there is a high probability that such Au is associated with secondary regolith carbonate. Weak Au-As mineralisation occurs in CBAC 142, along strike from the Muriel Tank mineralisation.

Mafic dykes occur in the rocks to the north and east of the Babinda Volcanics. These dykes can be enriched in chalcophile elements, including Co, Cu and Zn.

Mineralisation-associated elements may be present in Zn-rich profiles in the Babinda Volcanics, possibly analogous to the Mt Windsor Volcanics (in which stratiform mineralisation generally occurs at a particular level in the volcanic sequence). Weak As-Sb-Mo-W-Zn-(Cu)-(Au) mineralisation occurs in CBAC 167 and probably reflects the edge of more Pb-rich mineralisation.

CONTENTS

1 INTRODUCTION **1**

2 REGIONAL SETTING **2**

2.1 REGIONAL GEOLOGY 2
2.2 ECONOMIC GEOLOGY AND MINERALISATION 2
2.2.1 Mineral deposits in the Hermidale area 3
2.2.1.1 Quartz-vein type gold deposits 3
2.2.1.2 Stratabound metasediment-hosted copper mineralisation 3
2.2.1.3 Vein-type polymetallic mineralisation, Harts Tank Block 4
2.2.1.4 Polymetallic vein systems and disseminated mineralisation, Kopyje Block 4
2.2.1.5 Deposits associated with ultramafic intrusions 5

3 STUDY METHODS **6**

3.1 MAPPING 6
3.2 DRILLING, SAMPLING AND LOGGING 6
3.3 DATABASES 7
3.4 MINERALOGICAL ANALYSIS 7
3.5 DETAILED SOIL STUDIES 8
3.6 REGOLITH PROFILES AND SECTIONS 8
3.7 GEOCHEMISTRY 9

4 RESULTS AND DISCUSSION **12**

4.1 MAPPING 12
4.2 LOGGING 12
4.3 PIMA 14
4.3.1 Transported Regolith 14
4.3.2 Saprolite 14
4.4 DETAILED SOIL STUDIES 15
4.5 REGOLITH PROFILES AND SECTIONS 18
4.6 GEOCHEMISTRY 19
4.6.1 Mafic Profiles 19
4.6.2 Significant Au in the Saprolite 20
4.6.3 Significant Base Metal Contents in the Saprolite 20
4.6.4 Deep Transported Sequences 21
4.6.5 Regolith Carbonates 21

5 CONCLUSIONS **23**

5.1 REGOLITH ARCHITECTURE 23
5.2 GEOCHEMISTRY 23

ACKNOWLEDGEMENTS **24**

REFERENCES **25**

APPENDIX 1: DRILL HOLES NUMBERS AND SAMPLE INTERVALS **27**

APPENDIX 2: REGOLITH-LANDFORM MAPPING UNITS AND DESCRIPTIONS **28**

APPENDIX 3: DEPTH OF TRANSPORTED MATERIAL AND WATER TABLE FOR DRILL HOLES **30**

APPENDIX 4: ACID ATTACK ON DRILL HOLE SAMPLES **31**

APPENDIX 5: FIELD LOGS OF REGOLITH MATERIAL INTERSECTED IN DRILL HOLES **34**

APPENDIX 6: PIMA ANALYSIS LOGS **35**

APPENDIX 7: PALYNOMORPHS IN GREY CLAYS USED FOR DATING SEDIMENTS **39**

APPENDIX 8: GEOCHEMICAL DATA QUALITY AND RELIABILITY **40**

A8-1. ANALYTICAL PRECISION **40**
A8-2 LABORATORY PRECISION AND ACCURACY **40**
A8-3 SAMPLE REPRESENTATIVENESS **43**

APPENDIX 9: INVESTIGATION OF "REGOLEACH" ANALYSIS **47**

APPENDIX 10: GEOCHEMICAL DATA FOR THE HERMIDALE AREA **48**

APPENDIX 11: PIMA SPECTRA AND LOGS FOR THE HERMIDALE AREA **48**

1 INTRODUCTION

The Hermidale area is located between Nyngan and Cobar in central-western New South Wales, approximately 500 km northwest of Sydney. It is contained within the Cobar 1:250 000 sheet and covers the Hermidale 1:100 000 topographic map sheet and adjacent margins of the Canbelego, Sussex and Coolabah sheets (Figure 1).

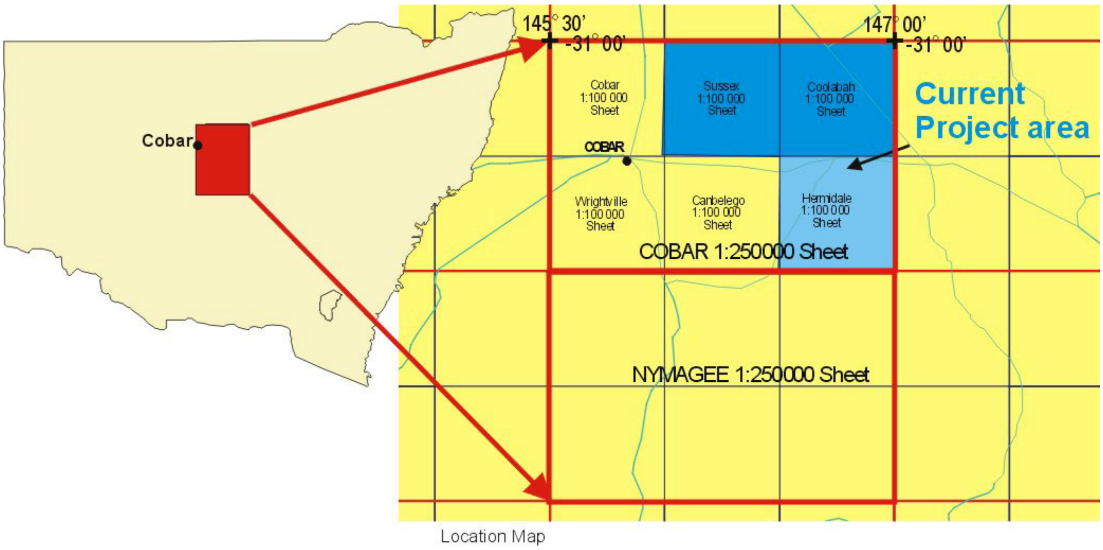

Figure 1: Location of the Hermidale 1:100 000 map sheet area in central west New South Wales.

The Hermidale area has a sub-arid climate with a mean maximum summer temperature (measured at Nyngan) of 34ºC (January) and a mean winter maximum temperature of 16ºC (July). The mean minimum temperature is 19ºC and 4ºC for summer and winter respectively (Bureau of Meteorology, 2002).

The aim of this study is to assist geological mapping and mineral exploration of the Girilambone Belt by providing a more detailed understanding of the geology and geochemistry of both the regolith and bedrock of the Hermidale area. The study is part of a series of projects being undertaken in conjunction with the NSW Department of Mineral Resources within the Girilambone Belt, covering the general area between Nymagee-Cobar-Bourke. A previously completed project covers the Sussex-Coolabah area of this region (Chan *et al.*, 2001).

A total of 49 air core drill holes (2275 m) along 5 road traverses across the Hermidale sheet area (Fleming and Hicks, 2002) were logged and sampled for geochemical and mineralogical analysis. Regolith-landform mapping and analysis of surficial materials were conducted in conjunction with the drilling program in order to provide a context for the drill hole data. Regional aeromagnetic and radiometric data were also integrated into the study to assist regolith-landform mapping, obtain information on subsurface regolith materials and plan drill hole positions. Parts of the Hermidale area, particularly the extensive alluvial plains in the northeast, contain thick regolith sequences and contrast with much of the regolith examined in the earlier Sussex-Coolabah project (Chan *et al.*, 2001). The current study provides additional insights into the regolith evolution and landscape history of the region. It also provides opportunities to assess geochemical associations related to regolith processes in background materials and geochemical dispersion processes adjacent to some mineralised sites.

2 REGIONAL SETTING

2.1 Regional Geology

Outcrop within the study area is generally highly weathered and very poorly exposed, commonly occurring as subcrop within creeks, roadside drainage and borrow pits. Large portions of the Hermidale 1:100 000 sheet area are dominated by flat, cultivated paddocks covered by alluvium.

The oldest outcropping rocks in the study area, and those that form "basement" are the Ordovician Girilambone Group. The Girilambone Group occurs as a north-trending belt through the region and is composed of strongly foliated, bedded and laminated quartz to quartzo-feldspathic sandstone, quartzite, shale, phyllite, chert, minor mafic volcanics and intrusives (Helix Resources NL, 1988). The lower turbiditic sequence of the Girilambone Group consists of interbedded metasandstones and phyllite, while the upper part is characterised by a turbiditic sequence comprising quartz-rich sandstone, siltstone, slate and chert (Gilligan and Byrnes, 1995). The chert beds occur either as thin layers interbedded with slate, or as mappable chert zones such as the Alandoon Chert, intersected within the Piesley Road (CBAC 178) and southern Nymagee Road (CBAC 171-172) drill traverses, where outcrops occur as prominent north trending ridges. The basement rocks of the Girilambone Group have been regionally metamorphosed to upper greenschist facies (Placer Exploration Ltd., 1991). Strongly deformed and boxwork quartz-veined micaceous quartzite and fine-grained sandstone (including the Budgery Sandstone member: Gilligan and Byrnes, 1995) outcrop as solid ridges at Rocky View Trig on the eastern end of the White Rock Road drill traverse (near Hermidale).

A number of drill holes on the southern end of the Nymagee Road traverse (CBAC 163-168) intersect the Silurian Harts Tank Beds at Rainbow Ridge. The Harts Tank beds comprise a complex sequence of fine-grained sandstone, siltstone, phyllite, black graphitic shale, chert, rhyodacitic to rhyolitic volcaniclastics, and minor altered andesitic lavas and tuffs (Pan Australian Mining Ltd., 1986). The widespread anomalous Cu, Pb, Zn, Au, Bi and in places W, Sb and Mo geochemistry of this sequence suggest a Silurian igneous association (Gilligan and Byrnes, 1995).

Major crustal extension in the latest Silurian to Early Devonian in the Cobar region led to the formation of a number of shallow water shelves (Gilligan and Byrnes, 1995). The shallow marine Kopyje Group is one such shelf, which developed on and adjacent to the Girilambone Group and borders the deeper water Cobar Basin (Planet Resources Group NL, 1988). The eastern part of the Kopyje Shelf, extending from north of Canbelego to Mineral Hill, south of Nymagee is characterised by a north trending zone of four magnetic centres. Within the study area, the Kopyje Group is represented by the Babinda Volcanics, which form a series of hills and peaks in the southwest corner of the study area, and the Florida Volcanics (east of Canbelego). The Babinda Volcanics were deposited mainly as ashflow and airfall tuffs, with minor rhyolitic to dacitic lavas and tuffaceous siltstones.

Known mafic rocks include serpentinised ultramafics at Miandetta in the east of the study area and the Honeybugle Intrusive Complex in the south east corner of the Hermidale 1:100 000 sheet. The Honeybugle Alaskan intrusive complex is a northwesterly trending body containing hornblende pyroxenite, hornblendite, serpentinite, melagabbro, syenodiorite, norite, monzogabbro and monzonite (Gilligan and Byrnes, 1995).

2.2 Economic Geology and Mineralisation

The Cobar-Girilambone-Nymagee region is one of the richest mineral provinces in New South Wales. The area covered in this study lies within this region, but no major deposits have yet been found. Major deposits occur in the Cobar Basin, just to the west, around Girilambone to the northeast, and at Canbelego and Nymagee to the west and southwest respectively. Deposits at these sites are described by Byrnes (1993), Suppel and Gilligan (1993) and Gilligan and Byrnes (1995). The major styles of mineralisation in the region are also summarised by Chan *et al* (2001). A number of small deposits and occurrences of base metals, gold and platinum group elements are known from the Hermidale sheet area and these are briefly reviewed in the following section.

2.2.1 Mineral deposits in the Hermidale area

Minor mineral occurrences and prospects are described from the Hermidale area in the Metallogenic Notes for the Cobar 1:250 000 sheet (Gilligan and Byrnes, 1995). These can be grouped into several deposit types as outlined below.

2.2.1.1 Quartz-vein type gold deposits

Deposits of the Muriel Tank goldfield belong to this style of mineralisation. The Muriel Tank goldfield is located just south of the Barrier Highway approximately 15 km west of Hermidale. The goldfield was developed in 1916 and produced intermittently from 1922-1936, a total of about 10 kg of gold (Gilligan and Byrnes, 1995). The goldfield consists of a cluster of about 10 separate workings over a NW trending area of 19 km^2. Aeromagnetic data suggest that this zone is localised along a regional fault system. Individual quartz-bearing reefs appear to be developed in shear zones and are near vertical, trending 340-350°. Distinct quartz veins, irregular veins, veinlets and masses of quartz as well as saddle reefs are reported. Most of the quartz is dark blue-grey with a resinous appearance (Jaquet, 1923, cited in Gilligan and Byrnes, 1995) and there is variable pyrite and possibly arsenopyrite associated with the gold. Individual veins may be up to 1.5 m wide with grades in some deposits over 30 g/t Au, possibly related to near surface supergene enrichment (Gilligan and Byrnes). The host rocks are phyllites and metagreywackes, considered to be part of the Girilambone Group. There is some evidence of disseminated pyrite in the surrounding country rocks. One of the air core holes (CBAC 142) drilled during the present study was located along strike, 6 km to the north of the Muriel Tank Goldfield and showed elevated Au values (20 ppb) in saprolite, accompanied by elevated As, Sb and Zn.

Individual deposits (with Cobar metallogenic map no.) include:

Toomeys reef (205)	Reef traced for 90 m at surface (production unknown).
Fettlers mine (206)	Quartz veins worked to 35m depth (recorded production 1.74kg Au).
Roach vein (207)	Narrow quartz vein with up to 20 g/t (no production)
Butlers mine (208)	Well-defined reef with up to 183 g/t Au and some Ag (recorded production 0.84 kg Au).
Russells mine (209)	
Unnamed (210)	
Golden Horseshoe (211)	Parallel quartz veins along cleavage (recorded production 5.2 kg Au).
True Blue, Blue lode (212)	Reef zone 1.3-2.2 m wide with grades up to 13.3 g/t
Mitchells mine (213)	
Browns Hope (214)	Narrow 25 cm thick vein with grades up to 63 g/t.

All the workings are reported to be shallow (deepest was Fettlers mine at 35 m).

2.2.1.2 Stratabound metasediment-hosted copper mineralisation

Copper mineralisation of this style occurs to the north of the Hermidale area at the major Girilambone and Tritton deposits. Mineralisation of similar style occurs at Budgery, just north of Hermidale. This is the largest known deposit on the Hermidale sheet with a total recorded production of about 1,500 tonnes of Cu and 63 g of Au. The total resource is estimated at 25,000 tonnes of ore grading 3.5% Cu (Gilligan and Byrnes, 1995). Most of the historic production appears to have come from the oxidised and supergene enriched zones. This has included leaching and extraction of copper from mine waters. The orebody is highly pyritic with lesser chalcopyrite in the primary zone. Secondary minerals developed include chalcocite, malachite, native copper, cuprite, azurite, goethite and jarosite. Gossans associated with the mineralisation contain up to 5 g/t Au. Mineralisation is developed near the folded contact between phyllites and psammitic schists with underlying chloritic, mafic schists. Quartz-magnetite rocks are associated with the mineralised horizon. The orebody is reported to have been pipe-like, pitching 40-55 SSE and up to 20 m wide (Gilligan and Byrnes, 1995).

2.2.1.3 Vein-type polymetallic mineralisation, Harts Tank Block

Small polymetallic vein systems are developed in the Harts Tank block in the southwestern area of the Hermidale sheet. These consist of multiple veins and disseminated mineralisation, generally hosted by felsic volcanic units in the Harts Tank Beds. They contain an association of Cu, Pb, Zn, Ag, and Au, with in some cases anomalous Bi, W, Sb and Mo. The mineralisation may be genetically related to intruded felsic plutons (Gilligan and Byrnes, 1995). Minerals reported include pyrite, pyrrhotite, magnetite, sphalerite, chalcopyrite, galena, tenantite, gold, scheelite and an unidentified bismuth mineral (Gilligan and Byrnes, 1995). Gangue minerals include quartz and calcite and there is associated silicification, sericitisation and argillic alteration. Hole CBAC 167 was drilled close to an example of this mineralisation (Road Shaft) and showed elevated levels of Zn, As, Bi, Sb, Mo and W.

Deposits recorded in the Cobar metallogenic notes (with Cobar metallogenic map no.) include:

Kypros Snake prospect (244)	Pb, Ag
Rainbow Ridge prospect (245)	Pb (Au, Zn, Cu)
Plumridge prospect (246)	Au (Bi)
Harts Tank Bi prospect (247)	Bi (Cu, W)
Upton (Harts Tank) prospect (248)	Zn, Pb (Cu, W)
Bills Retirement (249)	Au
Henrys Hill prospect (250)	Cu (Zn)
Henrys Hotel prospect (251)	Au
Road shaft prospect (252)	Pb (Zn, Cu)
Charlies Hope (253)	Au (Pb)
West Hudson prospect (254)	Au

2.2.1.4 Polymetallic vein systems and disseminated mineralisation, Kopyje Block

Felsic volcanic rocks of the Baledmund and Babinda Volcanics occur along the western and southwestern margins of the Hermidale area. These rocks host a number of small polymetallic deposits of multiple-vein, breccia-hosted and disseminated style. They contain Cu-Pb-Zn mineralisation with associated Au and Ag and have been variously described as of volcanogenic or epithermal origin (Gilligan and Byrnes, 1995: Golden Cross Resources, 2000). Ore minerals identified include pyrite, chalcopyrite, galena, spahalerite, gold, electrum, stromeyerite and tetrahedrite. There appears to be significant alteration associated with the mineralisation including silicification, chloritic alteration and carbonatisation.

Deposits in this group (with Cobar metallogenic map no.) include:

In the Baledmund Volcanics

Nerang prospect (196)	Cu-Pb-Zn
Kopyje prospect (199)	Pb-Zn-Cu-Ag
Glens Hill (200)	Cu-Pb-Zn-Ag
Pipeline Ridge prospect (202)	Cu-Pb-Zn-Ag-Au

In the Babinda Volcanics

Babinda Cu mine (241)	Cu (Au-Ag)
Lord Dudley (242)	Cu (Pb-Zn)
Babinda South (243)	Au-Cu

2.2.1.5 Deposits associated with ultramafic intrusions

The Fifield belt of Alaskan-type intrusive complexes extends into the eastern edge of the Hermidale area. These Alaskan-type intrusions are known to host platinum group elements in anomalous concentrations. They are also considered to be the source of placer platinum deposits worked in the Fifield area. Other bodies of serpentinised ultramafic rock have been described as Alpine-type affinity (Gilligan and Byrnes, 1995) but could also be highly deformed Alaskan-type bodies.

The Honeybugle Complex on the eastern margin of the Hermidale area contains several prospects with anomalous platinum associated with elevated Co, Ni, Cr and in some cases Cu, Zn, Au and Ag. Those described in the Cobar metallogenic notes by Gilligan and Byrnes (1995) are:

Honeybugle copper deposit (255)	An old copper occurrence with samples containing upto 2.6% Cu, 650 ppm Ni, 0.17 ppm Pt and 0.5 ppm Au.
Honeybugle North (256)	Old workings on an ironstone outcrop in weatheredultramafics, RAB samples average 0.54 ppm Pt over a 20 m wide zone.
Yarran Park (257)	Weathered pyroxenite with 194 m costean section averaging 0.34 ppm Pt and up to 1700 ppm Ni.
Mallee Valley prospect (258)	Pyroxenites and hornblendites, one RAB hole intersected 8m averaging 0.53 ppm Pt.

A significant Pt anomaly also occurs at the Gilgai prospect (220), 5 km south of Miandetta. Here a strong ferruginous weathering profile over ultramafic rocks contains up to 2 g/t platinum over an area of 700x200 m (Gilligan and Byrnes, 1995). Schistose serpentinite intercalated with phyllites at the Miandetta ballast quarry just north of Miandetta shows a similar ferruginous weathering profile and has been explored for potential lateritic Ni mineralisation.

Most of the ultramafic bodies outcrop poorly, but show strong magnetic anomalies. Four "bullseye" magnetic anomalies apparent in the aeromagnetics covering the Hermidale sheet area were investigated in the field as part of the current study. One of these is over the Budgery deposit, probably reflecting quartz-magnetite lode material associated with the copper mineralisation. Two sites (Magnetic Anomaly 1 at grid reference 475905E 6461943N and Magnetic Anomaly 3 at location 486054E 6506139N) showed no outcrop or distinguishing features at the surface, although gilgai soils were observed over Magnetic Anomaly 1. Several soil samples were collected from these two sites. Soil from Magnetic Anomaly 1 shows elevated Co, but two soil samples from different locations over Magnetic Anomaly 3 did not show any anomalous geochemistry. It seems likely that the magnetic feature is deeper than the overlying transported regolith. Investigation of the fourth anomaly (Magnetic Anomaly 2 at grid reference 470144E 6472500N) revealed float of ultramafic and pyroxenitic material in a dark-brown smectite-rich soil. Four soil samples from this site showed elevated levels of Co (up to 80 ppm), Ni (up to 750 ppm), and Cr (up to 2030 ppm). This site appears to be either a small Alaskan-type ultramafic intrusion or possibly an Alpine-type ultramafic body developed along a major fault. It has not been previously recognised and is worthy of follow up work. An air core hole (CBAC 185) drilled on the margins of a more diffuse aeromagnetic anomaly to the south, intersected weathered, laminated siltstones with anomalous gold values (25-85 ppb over 4 m).

In the present study anomalous gold values have been found in calcrete associated with ultramafic source rocks at Miandetta and Magnetic Anomaly 2.

3 STUDY METHODS

3.1 Mapping

The Hermidale 1:100 000 regolith-landform map (see back pocket of this report) covers the Hermidale 1:100 000 sheet as well as narrow zones on the three surrounding 1:100 000 sheets to the south, west and north. The map was constructed on the basis of Regolith-Landform Units (RLU's). RLU's provide a description of the relationship between dominant regolith types and their landscape setting. Regolith and landform types are described using a code system, which has specific latter combinations conveying the general information for each RLU (Pain *et al.,* 2002). For example:

Aap1

- The upper case letter/s (**A**) describe the main regolith type, (which in this case is alluvial sediments);
- The lower case letters (**ap**) describe the main landform type (which in this case is an alluvial plain), and;
- The modifier (**1**) is added to represent subtle differences within each RLU (for example, surface lag type, such as angular quartz clasts).

Initial discrimination of regolith-landform units was achieved through the use of aerial photographs (scales of 1:82 000 and 1:50 000), and remotely sensed radiometric, magnetic and DEM data. The methodology differed slightly from the production of the Sussex-Coolabah 1:100 000 regolith-landform map, in that more detailed air photographs were used (scale 1:50 000) for areas in which it was difficult to discriminate between regolith units at the scale of 1:82 000. A greater emphasis was also placed on interpreting the radiometric imagery, to aid in the discrimination between regolith-landform units.

The airborne digital data was supplied by NSW DMR and was acquired as part of the Discovery 2000 Initiative. Manipulation of the data in ArcView 3.2, ERMapper 6.1 and Intrepid 3.6 was done to enhance the imagery's detail, and included filtering, band manipulation, and production of magnetic derivative images (1.5VD). Confirmation of initial regolith-landform discrimination was gained through landform and regolith descriptions whilst in the field.

3.2 Drilling, Sampling and Logging

Drilling occurred along five main transects namely the White Rock, Gilgai, Peisley, Pangee and Hermidale-Nymagee roads (Figure 2). A total of 49 holes (2275 m) were drilled using a small 6-wheel aircore rig supplied by Geological Ore Search, Cobar. The drilling was conducted typically at 2-4 km spacing, but ranged from 1-8 km spacing. Depth of drilling ranged from 6-82 m. Prior to drilling at each new site, a hole two metres deep was drilled a few metres away from the intended drill site to purge the vacuum system in order to avoid cross-hole contamination.

Permanent reference chip tray samples were collected at every metre for the first 9 metres, then every 2 metres thereafter. Samples for geochemical analysis (approximately 4 kg) were taken every metre for the first 9 metres and then composite samples were collected until end of hole. Samples were also collected for palynological examination wherever possible, with a total of 20 samples being analysed.

A standard set of drill log sheets combining requirements for both CRC LEME and NSW DMR was used (as per Sussex-Coolabah drilling: Chan *et al*., 2001). The 49 field logs were logged by CRC LEME and have previously been reported by Fleming and Hicks (2002).

Upon return from the field, all 49 drill hole samples were logged in more detail using a polarising binocular microscope (Wild Photomakroskop M400). The detailed logging included characteristics such as Munsell colour, major minerals, carbonate content, magnetism, induration, sediment texture / grain size / roundness, and bedrock lithology. Such detailed logging enabled correlations to be made with the mineralogical information obtained from a PIMA (Portable Infrared Mineral Analyser), including definition of the transported/saprolite boundary, and aided understanding the whole rock geochemistry. Following the detailed logging, regolith material units were determined for all holes based upon the dominant regolith material/s (*i.e.*, sand, clay and gravel) to give profiles (see Section 3.6 of this report). Adjacent drill holes profiles were compared to give an indication of lateral variability between regolith profiles.

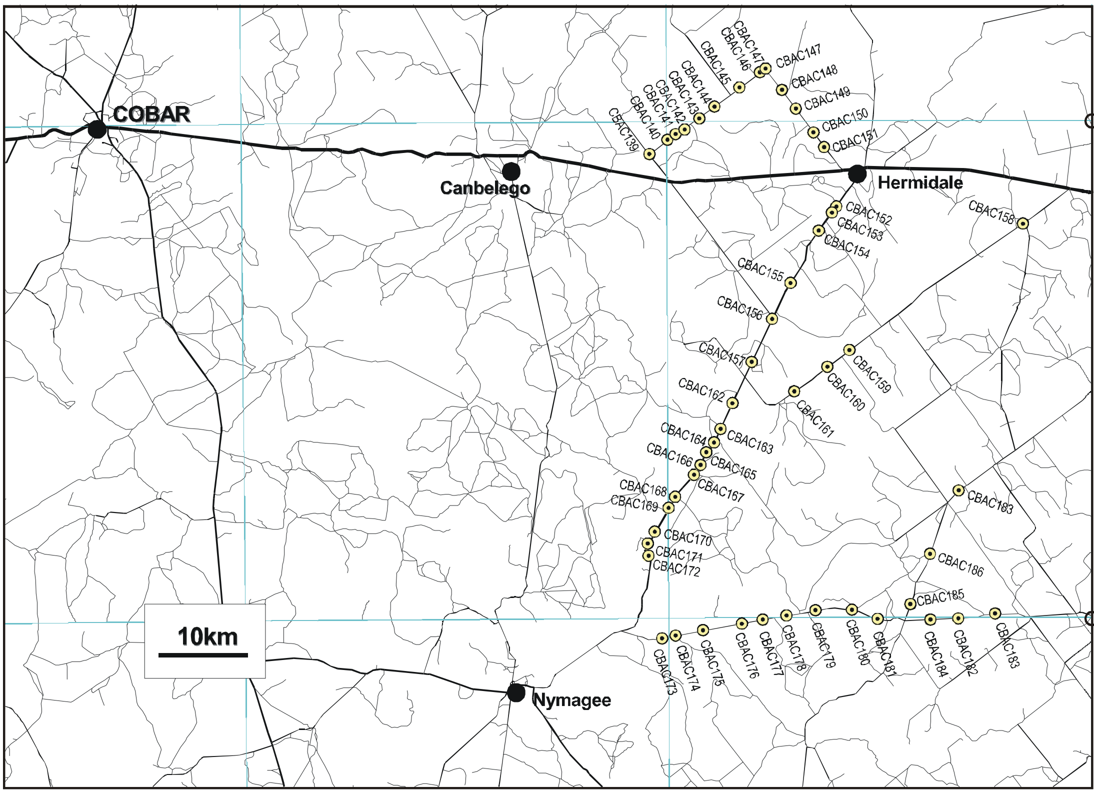

Figure 2: Location of the drill hole sites and traverses in the Hermidale area.

3.3 Databases

The location data, detailed regolith logs and geochemistry for the 49 drill holes were entered into the Geoscience Australia Regolith Database, Deviant. The location data were automatically imported into the Deviant Sites Table (Oracle) using Unix scripts. The location data correspond to the drill holes' Field ID (CBAC139 to CBAC187) and Geoscience Australia's ID (2001700139 to 2001700187). See Appendix 1 for the full list of IDs.

Field site information (including location data and site descriptions) was entered in the field geology database, OZROX. The location data contain both the Field ID (ZRC001 to ZRC031) and Geoscience Australia's ID (2001701001 to 20017010031). Also, seventeen regolith-landform unit descriptions were entered into the Regolith Database, RTMAP, for the Hermidale area.

3.4 Mineralogical Analysis

A PIMA II spectrometer was used to determine the mineralogy of material from all 49 drill holes from the Hermidale area. The PIMA instrument records the Short Wavelength Infrared (SWIR) reflectance spectrum (1300-2500 nm) of samples (Appendix 11). In this spectral region, discrete wavelengths of light are absorbed due to the bending and stretching of molecular bonds. The types of mineral groups which display absorption features within the PIMA range include phyllosilicates, hydroxylated silicates, carbonates, sulphates and ammonium-bearing minerals, plus Al-OH, Fe-OH, Mg-OH. Absorption features may overlap, *e.g.,* kandite minerals (kaolinite, dickite and nacrite) all have very similar Al-OH features and are difficult to distinguish spectrally. However, in most cases, experience allows the distinction to be made. Refer to Chan *et al.* (2001) for a more details on PIMA methodology.

Spectral Geologist (TSG) version 2 software has been used in the presentation and interpretation of the PIMA data for this report. TSG provides graphical interpretation by applying a series of algorithms to the spectra. In these samples, five algorithms have been used to display downhole changes in the regolith profile (Appendix 11). The algorithms used for this study are:

- Depth of the water peak (1880-1960 nm),
- Depth of the Al-OH peak (2180-2230 nm),
- Wavelength of the Al-OH peak (2180-2230 nm),
- Depth of the Fe-OH peak (2240 – 2280 nm and 2235-2245 nm), and,
- Kaolinite Disorder (Crystallinity) (2180/2160 nm).

For this report, PIMA data are provided as stacked spectra, and graphical interpretation as DOC files and TSG files.

Initially every second sample from each drill hole was analysed. Intermediate samples were measured, where appropriate, to help confirm the depth of the unconformity (transported sediments / *in situ* boundary).

The presence of acid-reactive components (mostly the carbonates, calcite and dolomite) was tested for each hole using concentrated HCl. Results were recorded as "M" for a major reaction, and "m" for a minor reaction, with samples containing no carbonate being left blank in the listing in Appendix 4.

X-ray Diffractometry (XRD) was used to determine non-phyllosilicate phases in selected samples (*e.g.,* to confirm the presence of feldspar and the nature of the carbonates).

3.5 Detailed Soil Studies

Four drill holes representing a range of regolith landscape units were sampled to better define the nature of the soil:

- Active Alluvial Plain: samples (1-5) at 1 m intervals from drill hole CBAC 152.

- Active Depositional Plain: samples (6-10) at 1 m intervals from drill hole CBAC 183.

- Erosional Plain: samples (11-15) at 1 m intervals from (CHep1) drill hole CBAC 160.

- Erosional Rise: samples (16-20) at 1 m intervals from (CHer1) drill hole CBAC 166.

A sample of each horizon was initially sieved through a 2 mm sieve to determine the gravel content. The electrical conductivity and pH was then determined on 1:5 soil-water extracts of the <2 mm fraction. In addition, the mineralogy of the bulk sample was determined using X-ray Diffractometry (XRD).

3.6 Regolith Profiles and Sections

Topographic profiles were derived from digital elevation data (DEM) from the NSW DMR Discovery 2000 Initiative, and constructed to scale with drill hole locations using Research Systems IDL (Interactive Data Language) software. Parts of the DEM data were missing (Figure 3), so the topographic profile was inferred (dashed line) from regolith-landform units in parts of Traverses 1 and 2. A standard scale with vertical exaggeration of 50 (horizontal scale of 1:50 000; vertical scale of 1:1000) was used for all five sections. The sections are in direct line between drill holes, which run along five road traverses:

- Traverse 1: White Rock Road
- Traverse 2: Nymagee -Hermidale Road
- Traverse 3: Gilgai Road
- Traverse 4: Peisley Road
- Traverse 5: Pangee Road

Regolith material units for all 49 drill holes were derived from interrogation of results of laboratory analyses (microscopy, PIMA, and acid attack) and compiled in appropriate locations along section lines (see back pocket of this report). Eighteen transported regolith material units and 13 *in situ* regolith material units were defined. The term "gravel" is used to encompass transported very coarse sand, granules and pebbles (1-64 mm). These regolith material units are attributed, where relevant, with specific clasts/lag, induration, vein and palynology details, as well as the water table where encountered. Regolith-landform unit intercepts and magnetic drainage sediment (see back pocket of this report, and Figure 4) intercepts are shown on all sections.

3.7 Geochemistry

Chemical analyses for Au (by *aqua regia* digest, solvent extraction and graphite furnace AAS analysis: method: AU-GF42) and 28 other elements using a combination of ICP OES and ICP MS following a multi acid digest (HF-HNO_3-$HClO_4$ digestion, HCl leach: methods ME- ICP61 and ME-MS61) were performed by ALS-Chemex Laboratories in Orange. All samples collected during the project were analysed by this approach because of the low cost and its wide use by exploration companies working in the region. Our assessment is that while this is not a “total” analysis technique for a number of elements, it gives a good first pass indication of element abundances, particularly for most (but not all) elements of direct interest as commodities or pathfinders (see also Appendix 8). Geochemical data for the Hermidale area is listed in Appendix 10.

Bottom of the hole samples were also analysed by major and trace element XRF techniques at Geoscience Australia, to assist in lithological identification. This provided more satisfactory results for some major elements and a number of minor and trace elements, such as Ti, Cr and Zr, hosted in insoluble or partly soluble minerals. These immobile elements are commonly used for discrimination of major rock suites.

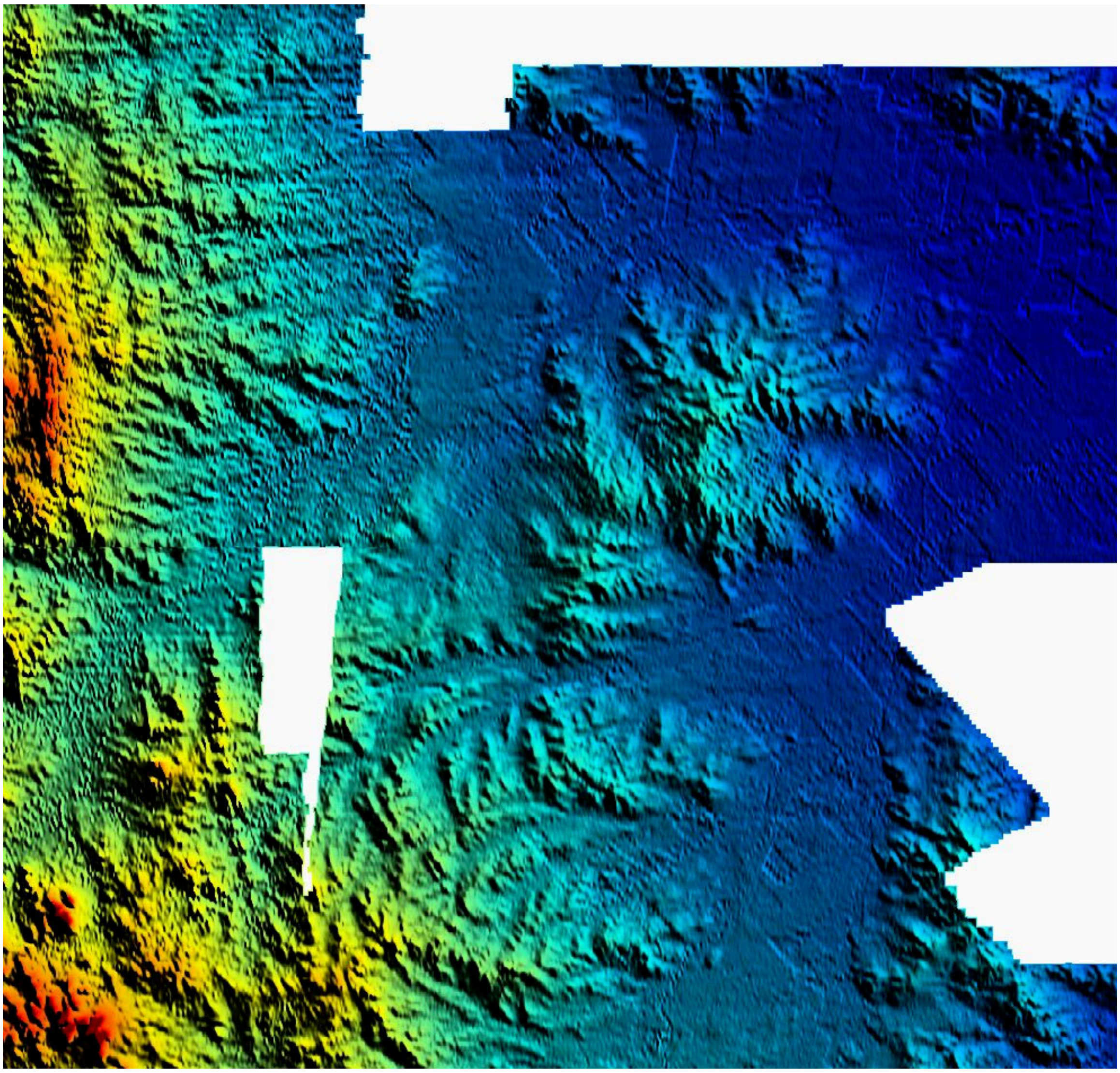

Figure 3: Digital elevation model (DEM) of the Hermidale area (with northeast sun angle filter). Gaps in data are due to mining lease restrictions.

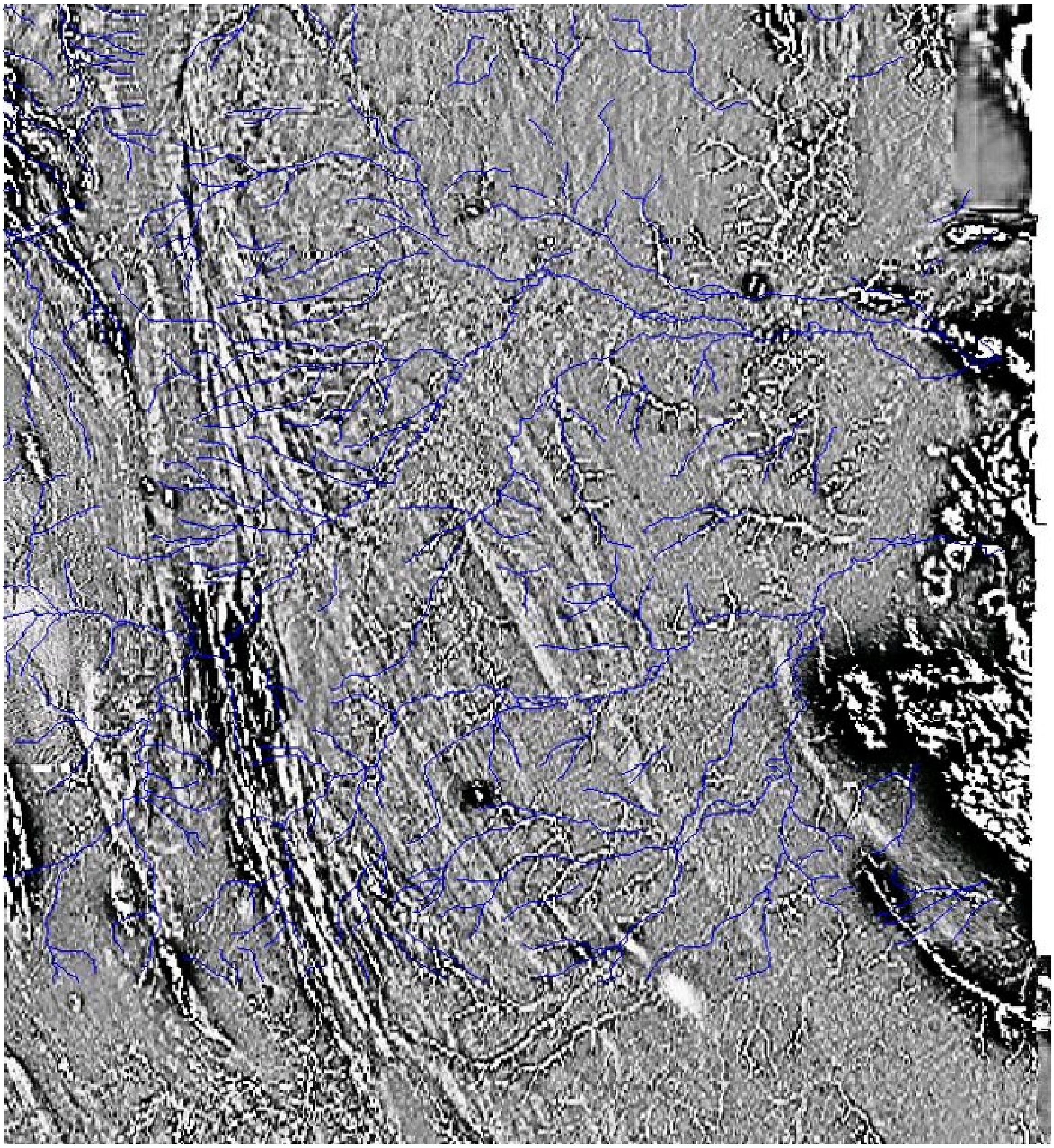

Figure 4: 1.5 vertical derivative magnetics imagery of the Hermidale area showing magnetic drainage lines and magnetic basement. Present day drainage is in blue (except for strip along the southern border of the image).

4 RESULTS AND DISCUSSION

4.1 Mapping

The regolith-landform map for the Hermidale area was produced at 1:100 000 scale and has seventeen regolith-landform units, which encompass alluvial and colluvial units with depositional/erosional processes, and saprock units (see regolith-landform map in back pocket of this report). The regolith-landform units are described in Appendix 2.

Sediments cover plains and rises over most of the Hermidale area. All but one of the alluvial units (Aed1) are associated with the Whitbarrow and Pangee Creeks corridors, located in the northern and eastern parts of the area. The alluvial units generally reach depths of between 5 and 40 m of transported sediment. The units include alluvial channels (ACar1, ACar2), alluvial plains (Aap1, Aap2, Aap3) depositional plains (Apd1, Adp2) and an alluvial fan (Afa1). Differentiation between alluvial channels, alluvial plains and depositional plains was facilitated by interpretation of the Hermidale radiometric image (Figure 5). Alluvial unit Aed1 is widespread forming dendritic erosional depressions, dominantly within colluvial erosional plains.

Colluvial regolith-landform units are widespread across the Hermidale area with the higher relief unit (CHer1) occurring in the southwest. The colluvium associated with these units has a general depth of less than 5 m, with surface material consisting of quartz and maghemite. The colluvium overlies saprolite, and in places palaeovalley sediments, especially in CHep1 (see section 4.5). The DEM (Figure 3) and topographic maps were used to help differentiate between plains, rises and low hills for both colluvial and saprock units, showing the variation of relief in the area to be between 1 m and 90 m.

In situ units of exposed saprock (slightly to moderately weathered bedrock) on plains, rises and low hills occur in the west and southwest of the Hermidale area. Interpretation of the radiometric image (Figure 5) shows these units to have a high radiometric response in all channels relating to outcropping acid volcanics.

4.2 Logging

The depth of the transported/saprolite boundary for the 49 holes varied according to bedrock lithology, landscape position and the presence of buried palaeovalleys. In the Hermidale study area, the depth of this boundary changed markedly from 1-3 m in bedrock dominated holes (in units CHer1 and CHep1) to an average depth of around 20 m for palaeovalley dominated holes (in units Aap1, Apd1 and 2). A full list of the transported/saprolite boundaries can be seen in Appendix 3.

The lithology/mineralogy of the transported materials also varied throughout the study area. Within the bedrock dominated holes in regolith-landform units CHer1 and CHep1, transported materials were commonly shallow (< 3 m) and consisted of red/brown silt, sand and clay with minor sub-rounded to sub-angular quartz and magnetic granules to pebbles. However, transported materials intersected in drill holes within the palaeovalley sediments were deeper and lithologically more varied. These materials consist mainly of sands, brown clay, grey clay, magnetic gravels, lithic gravels, or a combination of all these materials, and occur within regolith-landform units CHpd1, Aap1 and Apd1 and 2. Compared with the transported sediment packages found in the Sussex-Coolabah area, the sediments found in the Hermidale area are best considered as mixed sediment packages rather than discrete units (*i.e.,* clay, sand, gravel).

Changes in the bedrock lithology are not as varied as those shown by the transported materials. The dominant lithology throughout the Hermidale area was phyllite/siltstone, with sandstone, chert, volcanics and black graphitic shale occurring as minor lithologies. One quarter of the holes drilled (12 holes) encountered both phyllite/siltstone and sandstone within the same hole. Bleached saprolite was noted in 11 holes (from both bedrock dominated and palaeovalley holes) and consists entirely of kaolinite and minor quartz veining (see Section 4.5 in this report).

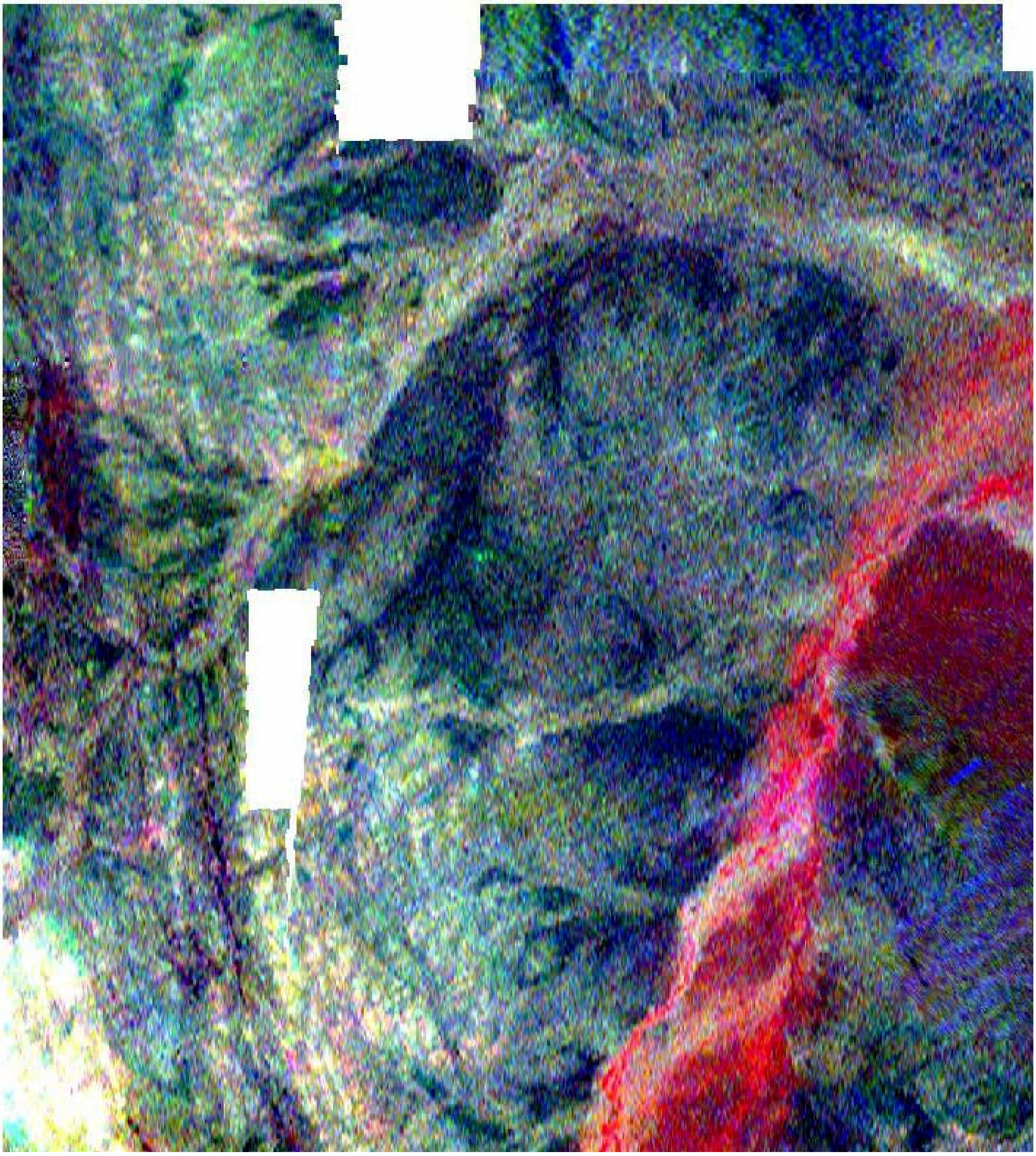

Figure 5: Radiometric image of the Hermidale area (red - high K, green - high Th, white - high in K+Th+U. Note the granite-sourced alluvium from south of the area along Pangee Creek. Gaps in data are due to mining lease restrictions.

The water table was intersected in 14 holes during the drilling. The depth of intersection of the water table ranged from 33 m (CBAC 173) to 67 m (CBAC 160). In all cases, the water table was beneath the transported regolith (Appendix 3).

Evidence of secondary cementation in regolith chips was not commonly encountered during the logging (see Section 4.5 in this report).. However, silicified saprolite chips mainly occur in CBAC 164, 177 and 180 at depths ranging from 2 m to 39 m. Minor silicified saprolite occurs in CBAC142, 162, 168, 174, 175 and 176, with silicified sediments also in CBAC162 and 174. Ferruginous saprolite mainly occurs in CBAC168 and 177 from 0 to 29 m depth, and minimally in CBAC180. Ferruginous indurated chips were found within transported regolith in CBAC 155, 156, 171, 179, 181, 182, 186 and 187 at depths from 4 m to 13 m.

Results for acid reaction with HCl (Appendix 4) indicate that reactive carbonate is prominent throughout the study area (with only one hole out of the 49 showing no reactive samples). Carbonate is prominent in the upper saprolite and overlying transported material within some holes (*e.g.,* CBAC 141, 145, 150-151, 159, 162, 163, 169, 171-173 and 176). However, in other cases, carbonate is only present in the saprolite (*e.g.,* CBAC 142, 143, 149, 175 and 178) of transported material (*e.g.,* CBAC 144, 146, 148, 152, 157, 179, 181-184 and 187). The presence of elevated Ca and Mg in many of these carbonate-bearing samples suggests that dolomite may commonly be the dominant carbonate phase (*cf.* Appendix 10).

4.3 PIMA

The spectra indicate there are some general mineral assemblages that can be seen within both the transported regolith and the saprolite. The associations are:

- Transported Regolith – Kaolinite ± Illite ± Smectite

- Saprolite – Kaolinite ± Muscovite/Phengite ± Illite ± Smectite

4.3.1 Transported Regolith

PIMA results are used to help define to the unconformity, and aid identification of clay minerals within the transported regolith. The common clay minerals identified were kaolinite, illite and smectite.

4.3.2 Saprolite

The saprolite in the Hermidale area is commonly derived from the weathering of siltstone/phyllite and sandstone, with volcanics locally important in the west-southwest of the study area. There is also an indication of weathered material from mafic intrusions, most probably mafic dykes.

The most common mineral assemblage was kaolinite + muscovite ± phengite, which accounted for approximately half of the holes analysed (Appendix 6A). Less common mineral associations include:

- Kaolinite + Phengite (CBAC 151, 152, 159, 161), (Appendix 6B);
- Kaolinite + Muscovite ± Smectite (CBAC 145, 167, 171, 172, 173) (Appendix 6C); and,
- Kaolinite + Muscovite ± Illite (CBAC 141, 165, 169, 170, 175, 177, 178) (Appendix 6D).

Mafic material (most probably mafic dykes) has been located within five holes in the Hermidale area (CBAC 163, 8-9 m and 33-45 m, CBAC 165, 3-8 m, CBAC 166, 3-27 m, CBAC 176, 39-41 m and CBAC 179, 15-17 m). The mineralogy of the mafic saprolite commonly shows kaolinite as the dominant clay mineral, with deep absorption features for the Fe-OH peak (although not all mafic saprolite shows this feature) which is generally indicative of ferromagnesian bedrock (Appendix 6E). In CBAC 166 (despite elevated Cr contents suggesting a mafic origin), the PIMA was unable to recognise any phyllosilicates and therefore gave a Null/Null response (Appendix 6F).

Contrasting with these general features, CBAC 174 displays the deepest absorption features for the Fe-OH peak but contains the most felsic rock (Ti/Zr=4) from within all the holes drilled (Appendix 6G).

CBAC 154 is a good example of how the PIMA is used to help define the transported/saprolite boundary. It shows a clear boundary at 11m, highlighted by a marked change in the depth of the water and kaolinite crystallinity algorithms (Appendix 6H).

4.4 Detailed Soil Studies

Figures 6-9 show the electrical conductivity (EC) *versus* pH profiles for four different regolith landform units. Below 1 m all profiles showed a marked increase in EC and pH. The EC typically increased from < 0.1 dS/m in the upper 1m to 0.4-0.6 dS/m at 4-5 m depth. The pH also increased from 5.5-6.5 in the upper 1 m to > 8.0 at 4-5 m, with values as high as 9.5-9.6 being recorded at intermediate depths.

These higher values of EC and pH, well below the current surface, indicate a substantial accumulation of salts in the profile of all four regolith landforms. From the high pH values, these salts are interpreted to be mainly carbonates (See Appendix 4).

Further work is currently underway to determine the mineralogy and other properties of these soluble components and to establish their origin (*viz.,* could they be aeolian?).

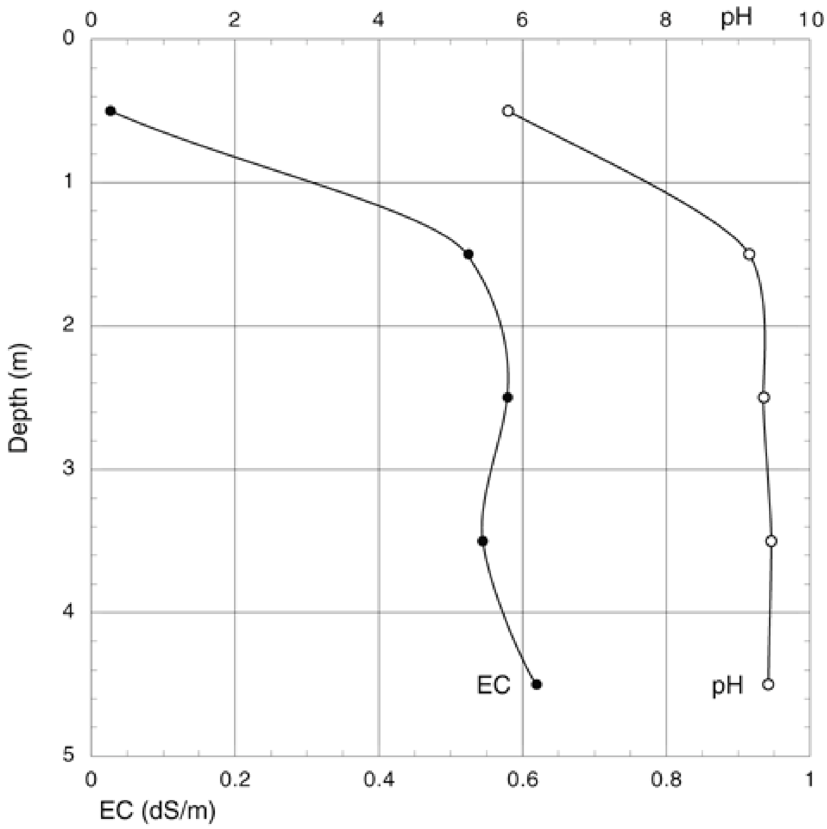

Figure 6: Active Alluvial Plain: samples at 1 m intervals from drill hole CBAC 152 (transported material to 35 m).

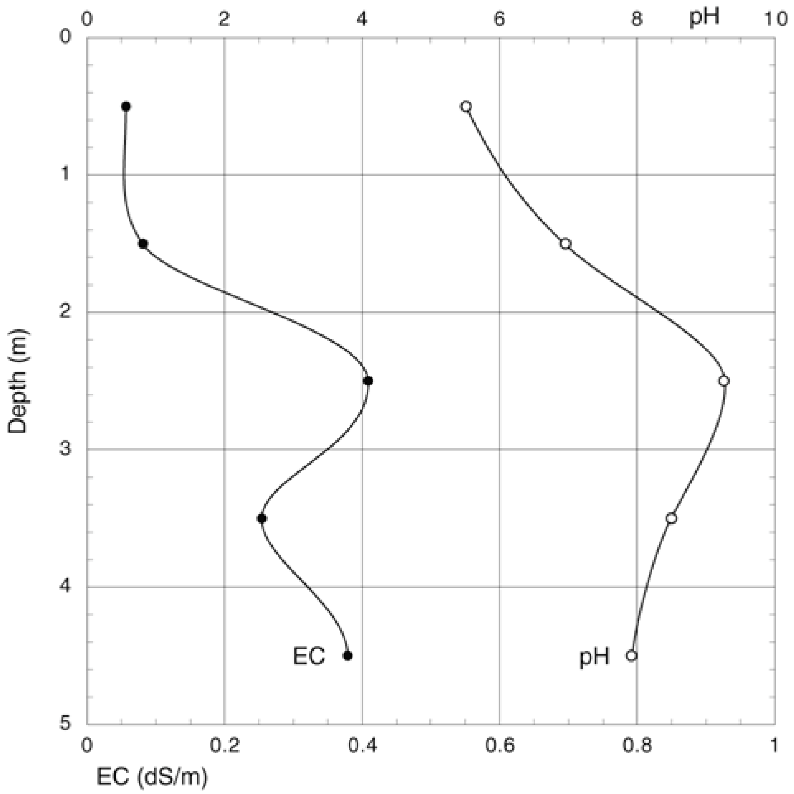

Figure 7: Active Depositional Plain: samples at 1 m intervals from drill hole CBAC 183 (transported material to 35 m).

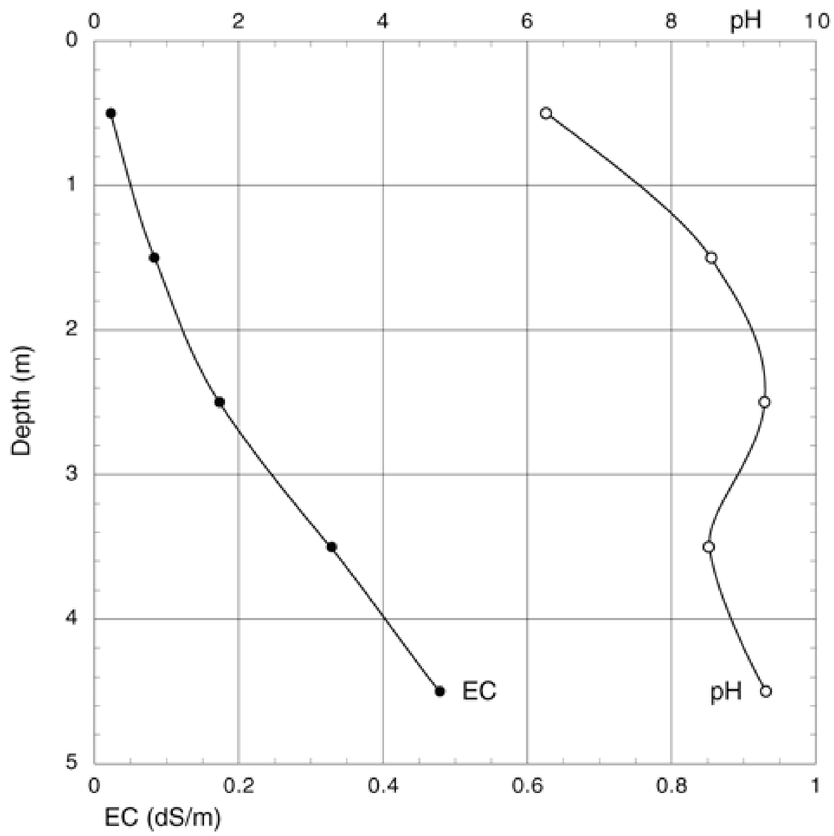

Figure 8: Erosional Plain: samples at 1 m intervals from (CHep1) drill hole CBAC 160 (transported material to 13 m).

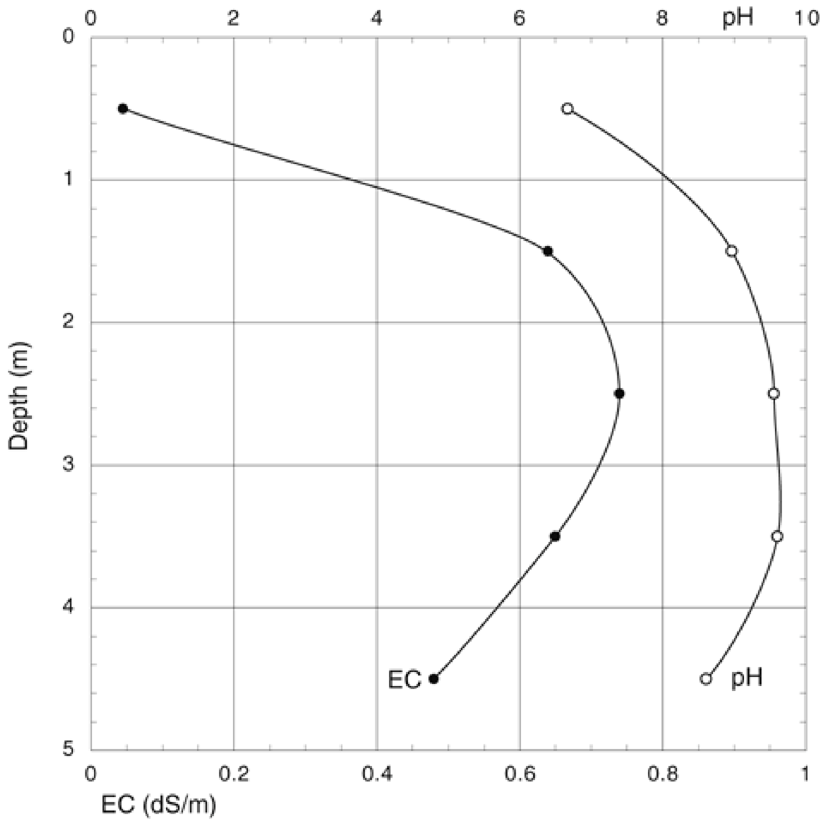

Figure 9: Erosional Rise: samples at 1 m intervals from (CHer1) drill hole CBAC 166 (transported material to 2 m).

4.5 Regolith Profiles and Sections

Regolith profiles for all drill holes are displayed in their true topographic position along the five sections (see back pocket of this report). Interpolation between drill holes was not attempted because the drill holes were spaced too far apart (typically 3-4 km) relative to the lateral variability of regolith material units for a meaningful interpretation of profile continuity along the sections.

The topographic profiles for the five sections show a general reduction in elevation towards the east, with an increase in gradient towards the east in four of the sections:

- east of CBAC144 on Traverse 1;
- 1 km east of CBAC 168 on Traverse 2;
- 11 km east of CBAC 159 on Traverse 3; and
- 1 km east of CBAC 177 on traverse 4.

There is also a general reduction in relief towards the east from around 20 m in the west to less than 5 m in the east. Erosional plains and rises are dominant in the west, whereas depositional plains are dominant in the east.

Regolith profiles in the erosional domain to the west generally have only 1-2 m of sediment over saprolite, but some drill holes (CBAC 148, 157, 160, 161, 170, 179 and 180) have sediment up to 15 m depth. These greater depths of sediments indicate palaeovalleys. Regolith profiles in the depositional domain to the east have a greater thickness of sediments, to over 42 m depth in CBAC 158, and vary considerably in depth between neighbouring drill holes (*e.g.,* 11 m in CBAC 154 and 35 m in CBAC 152). This indicates a more rugged palaeotopography than the present alluvial plain.

Sediment units are defined by the relative abundance of gravel/sand/silt/clay. Units include those with composite dominant materials, which are more common, and units with a dominant single material and other minor (<10-15%) materials. The latter is shown as single materials in the legend for the drill hole profiles and sections (see back pocket of this report). Silt is apparently ubiquitous (from microscopic analysis) in the top 2 m layer of sand and brown clay, plus gravel in places, on both underlying saprolite and sediments. However more detailed particle size analysis is required to confirm this. Sediments are distinguished from being reduced or oxidised by the presence of grey or brown clay respectively. Reduced sediments are dominant and usually occur beneath 1-9 m of oxidised sediments. Basal gravels and sands are common above reduced clays (CBAC 146, 152, 153, 157, 160, 161, 179, 180, 185, 186, and 187. Minimal grey clay occurs in the basal 4-13 m sand and gravel unit in CBAC 154, perhaps indicating erosion of the grey clay from elsewhere. More detailed sampling (1 m intervals from surface to the sediment/saprolite interface) may be required in future drilling to facilitate adequate facies interpretation.

Palynological age determination was attempted on samples from 10 drill holes. Age determination was difficult due to the high percentage of contaminant elements, the scarcity of palynomorphs, and the long range of assumed *in situ* taxa (E. Monteil, pers. comm., 2002). Dates were obtained in five drill holes from six palynomorphs found in reduced clay units (Appendix 7):

- CBAC154
  2-4 m in grey clay and sand unit: mid Palaeocene - Early Pliocene
- CBAC 181
  3-4 m in grey clay unit: since Late Jurassic - freshwater environment
- CBAC182
  1-2 m in grey clay unit: mid Palaeocene - Early Pliocene
  2-3 m in grey clay unit: mid Eocene - Pliocene
  5-7 m in grey clay, sand and gravel unit: mid Palaeocene - Early Pliocene
- CBAC184
  4-5 m in grey clay unit: mid Palaeocene - Early Pliocene
  8-9 m in grey clay unit: Late Miocene – Quaternary
- CBAC 185
  8-9 m at base of grey clay unit above saprolite unconformity: mid/Late Miocene - present

The tightest inferred age range of Late Miocene to Early Pliocene is indicated by the two dates from CBAC 184. This correlates with the Lachlan Formation in palaeovalleys associated with the Lachlan River system, as well as correlatives in the Macquarie River system to the southeast. The Lachlan Formation is interpreted to have been deposited in a reduced environment and has an erosional contact with oxidised sediments of the overlying Cowra Formation (Williamson, 1986).

Magnetic imagery of the Hermidale area (Figure 4) shows dendritic drainage systems containing magnetic sediments. These systems broadly relate to the trends of the present drainage systems, but differ in detail, thus indicating that the magnetic sediments relate mainly to palaeodrainage. The more obvious palaeovalleys with magnetic sediments are shown as intercepts on the five sections. Most of the palaeovalleys with magnetic sediments occur within regolith-landform units CHpd1, Aap1, Apd1 and Aed1, with lesser occurrences within ACar1. In detail magnetic palaeosediments occur dominantly under present sloping sheetwash plains (both eroding and depositing) and alluvial plains, with less coinciding with present depressions and drainage lines or topographically inverted on crests. Magnetic material in the drill holes are mainly sands, and, to a lesser extent, gravels. Some drill hole sediment profiles have minimal or no magnetic material and do not relate to the magnetic imagery, *e.g.,* CBAC 184, 185 and 187, indicating the palaeosediments are more extensive than their obvious extent on the 1.5VD magnetic image (Figure 4).

Saprolite is penetrated in all drill holes except drill holes CBAC 153 and 158. Highly weathered bedrock extends to at least 82 m (CBAC 154). Four drill holes also penetrate saprock (CBAC 143, 149, 167 and 182). Phyllite/siltstone, sandy phyllite and sandstone are the dominant bedrock lithologies, with minor volcanics (CBAC 163, 166 and 167), chert (CBAC 174 and 178), and black shale (CBAC 168). Saprolite with indeterminate lithology is encountered in CBAC 179 and 187. Bleached saprolite occurs directly beneath sediments in CBAC 143, 145, 152, 156, 157, 160, 161, 172, 175, 178 and 182, and further down the profile in drill holes CBAC 142, 146, 154, 155, 163 and 175. Vein quartz is common, especially in CBAC 141, 145, 147, 154, 160, 163, 172, 174, 176, 178, 180 and 185.

Silicification is more common than ferruginisation, but not widespread. Silicified saprolite occurs mainly in drill holes CBAC 164, 177 and 180, and ferruginised saprolite mainly occurs in CBAC 168 and 177. Carbonate occurs in most of the drill holes and is commonly associated with the transported/saprolite interface or sediments higher in the profile (see Section 4.2 and Appendix 4).

4.6 Geochemistry

4.6.1 Mafic Profiles

Samples with Cr contents ≥200 ppm are observed in holes CBAC 163, 165 and 179. The previous study considered such material as mafic dyke material (Chan *et al.*, 2001). In CBAC 163, such material occurs between 8-9 m (upper saprolite) and from 33-45 m (lower saprolite) and is associated with elevated Ti>1.2 %, Fe>8 %, Mn>1000 ppm, P>3000 ppm, Sr>500 ppm and V>200 ppm, although the more highly weathered material at 8-9 m has lower P and Sr contents (Appendices 6I and 9). Similarly the 15-17 m interval in CBAC 179 has elevated abundances of these characteristic elements but lower P and Sr (Appendices 6E and 9) *i.e.* P and Sr are more liable to be leached during sustained weathering than the other characteristic mafic indicator elements. X-ray diffraction analysis of upper and lower saprolite material from CBAC 163 suggest that these elements may be hosted by apatite, which is destroyed as weathering proceeds. The position of the weathered mafic material immediately below the transported/residual interface in CBAC 179 may imply that the mafic dykes are highly susceptible to weathering.

In the intervals, 2-27 m in CBAC 166 and from 39-41 m in CBAC 176, Cr contents are much lower but Ti, Fe, Mn, P, Sr and V are all high (Appendices 6F, 6J and 9). Thus it appears likely that the acid dissolution technique, used prior to chemical analysis (Section 3.7 and Appendix 8), may not always completely dissolve the Cr minerals in mafic rocks. Possibly this may imply the presence of a resistant Cr-mineral (*e.g.* chromite) in these two drill holes and less resistant Cr-bearing minerals in other mafic samples. Whether this is true or not, it does suggest that Cr by itself is not reliable as an indicator of mafic dykes, and that elevated Ti, Fe and V should also be considered.

The PIMA spectra of these mafic intervals are characterised by strong water development features and low abundances of clay minerals (Appendices 6F and 6I). Commonly the TSA algorithm was unable to identify any phyllosilicate phases although X-ray diffraction indicates smectite + trace kaolinite in such samples. Sometimes the depth of the Fe-OH feature readily identifies the presence of mafic intervals (*e.g.* Appendix 6E).

4.6.2 Significant Au in the Saprolite

Elevated levels of Au (≥5 ppb), generally with significant As, occur in holes CBAC 142, 154, 159 and 175. The most consistent of these occurrences is in CBAC 142 from 29-48 m where up to 21 ppb Au occurs and As contents are generally>20 ppm. Below 29 m other geochemical data, particularly Fe but also Al, Cu, Ti and Zn are elevated (Appendices 6K and 9). From 39 m downwards, Zn tends to be further elevated relative to abundances higher in the profile. The PIMA spectra also suggest a decrease in the kaolinite crystallinity and an increase in the abundance of mica at about 29 m. The amount of transported material in this profile is low and dolomite, reflected by elevated Ca, Mg and Sr contents, is strongly developed at the top of the residual saprolite (especially between 1-3m). There may be some enrichment of Au associated with the carbonate in that interval (Appendix 6K).

In CBAC 154, detectable Au (5 ppb) occurs in two samples between 8 and 33 m depth. These occurrences are unaccompanied by other potential pathfinder elements although elevated As (>20 ppm) does occur intermittently from 47-82 m *i.e.* lower in the profile. The PIMA spectra clearly indicate the transported/saprolite boundary at 11 m, and hence that the upper anomalous Au sample occurs towards the base of the transported material (Appendix 6H) and may imply a nearby source. Although carbonate is only weakly developed in the profile, the presence of 4 ppb Au in the upper metre (Appendix 6H) may be significant.

In CBAC 159, Au ≥4 ppb occurs in the top 3 m and from 19-27 m. However, as in CBAC 154, elevated As occurs in different samples (from 3-9 m: Appendix 6B). Carbonate, reflected by Ca, Mg and Sr contents, is strongly developed between 1 and 6 m (Appendices 6B and 9). Thus, it is also possible that the Au in the transported material in the upper 2 m of this profile is, at least, partly associated with carbonate.

CBAC 175 contains As>20 ppm throughout (0-37 m) but anomalous Au only occurs from 25 m downwards with 22 ppb occurring in ferruginous material from the bottom of the drill hole. Anomalous W (16 ppm) and high Zn (470 ppm) also occur in that sample(Appendix 10). Lead (and Bi) contents also tend to be elevated through the profile (Appendix 6L). Although some carbonate is present down to 9 m, carbonate is not strongly developed at the transported /saprolite interface at 1m (Appendix 6L).

4.6.3 Significant Base Metal Contents in the Saprolite

Substantial As, Sb, Cu, Mo, W and Zn contents occur through the length of CBAC 167 through the Babinda Volcanics, with isolated anomalous Au also present at the top and bottom of the hole (Appendices 6M and 9). Zinc contents are particularly high (1400 ppm) toward the end of the hole at 21 m and maintain abundances >700 ppm up to 7 m. PIMA spectra also show a change from dominant illite to kaolinite above this level (Appendix 6M), and indicate that the decrease in Zn content reflects dispersion of mobile elements with intense weathering. Some carbonate is developed at the transported/saprolite interface, with the increased Ca below 15 m reflecting the presence of residual plagioclase in lower saprolite/saprock. Dump material from an old shaft, 30 m away from this hole, contains 1.8 % Pb plus anomalous Au, As, Cu, Mo, Sb, W and Zn (M. Hicks, pers. comm. 2002) and hence this hole must be regarded as representing the edge of a mineralised zone.

Significant Zn (>100 ppm) is present below 3m in CBAC 174 and below 11 m in CBAC 176 (Appendices 6G and 6J). In the former case, this distribution represents the thickness of the residual saprolite and Zn is accompanied by Mn (>1000 ppm, Appendix 10). The highest Zn contents occur closest to the unconformity. However, in CBAC 176, Zn abundances increase down the profile, reflecting normal dispersion of Zn during weathering (as in CBAC 167), although the greatest Zn content is associated with Co, Mn, Ti, Fe and P within a mafic dyke (see Section 4.6.1

above). PIMA spectra indicate a change from muscovite/phengite- to kaolinite- rich assemblages above 7 m *i.e.* close to where the Zn anomalism stops (Appendix 6J). This coincidence again suggests that Zn is depleted as weathering intensity increases. In fact, because muscovite (and phengite) may contain hundreds of ppm Zn (*e.g.* Scott, 1988) but kaolinite does not, the destruction of its host may be responsible for its depletion higher in the profile. Carbonate is present at the transported/residual saprolite interface in this hole. The presence of intermittent anomalous Bi and/or W with the elevated Zn in both these holes (Appendix 10), indicates that this region within and about the Babinda Volcanics (including hole CBAC 167 which has been seen to be weakly mineralised) in the southwest of the study area deserves further investigation for its mineral potential.

CBAC 168 passes into black carbonaceous shale which contains pyrite at 47 m. Although the S contents of the material below 47 m is elevated to >1% in the basal sample and the chalcophile elements, Co, Cu, Ni and Zn are intermittently elevated (Appendix X), there is no indication that these elements represent anything else than the result of weathering of barren pyrite. Carbonate, reflected by Ca abundance, is present in the upper 3 m of transported material in this profile. The PIMA spectra reflect the major change at 49m with muscovite dominance giving way to deep Fe-OH feature-dominated spectra, possibly reflecting residual chlorite below 47m (Appendix 6N).

4.6.4 Deep Transported Sequences

Profiles from CBAC 183 and 187 pass through 35 and 36 m of transported material respectively. Spectrally this transition is much more evident in CBAC 187 (Appendices 6O and 6P). The profiles show considerable spectral variation between gravels and clays, consistent with derivation of material from several sources or at different times (see Section 4.5).

4.6.5 Regolith Carbonates

Previous studies (*e.g.* Lintern and Butt, 1998) have established an association between regolith carbonate (calcrete) and gold in the semi-arid regions of southern Australia. Calcrete has also been suggested as a useful sampling medium for gold and gold-base metal exploration in southeastern Australia (Hill *et al.,* 1999; McQueen *et al.,* 1999). Study of regolith material from the Hermidale area has revealed the widespread occurrence of carbonate in the upper part of the regolith profile (Appendix 4) and the geochemistry of bulk samples (Appendix 10) confirms the association of Au.

As part of the Hermidale study, calcrete samples were collected from available exposures or from the soil, and analysed for Au plus a suite of other elements. These samples were mostly collected from farm dams and borrow pits and included nodular, pedogenic and laminated or bedrock-coating facies. Several samples (including Mag An2) were collected around uprooted trees. Most of the calcrete samples showed Au concentration at or below the detection limit (1 ppb). Several samples were above detection but below what is considered a regional Au threshold for anomalous values (4 ppb). Four calcrete samples had Au contents above the regional threshold (Figure 10). These included samples from soil over an ultramafic intrusion at Magnetic Anomaly 2 (Mag An2 with 13 ppb), a sample of bedrock-coating calcrete on ultramafic schists at the Miandetta Quarry (Miandetta with 140 ppb) and two samples from an area of known base metal mineralisation (CBAC 167, Road Shaft prospect, with 4 and 5 ppb).

Interestingly, the data suggest high background gold associated with the ultramafic rocks in the Hermidale area.

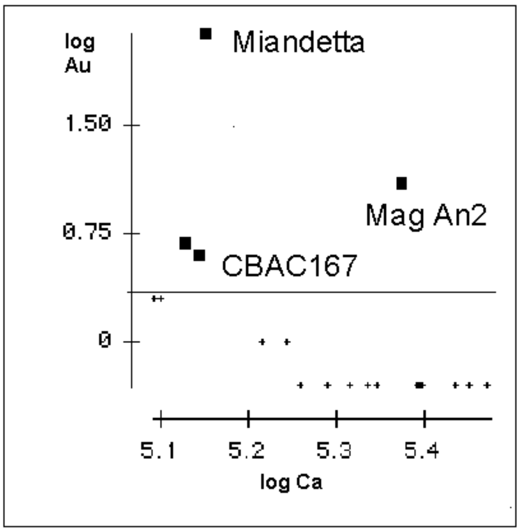

Figure 10. Concentration of Au (log ppb) versus Ca (log %) in calcrete samples collected from the Hermidale area. Horizontal line is regional threshold.

A plot of Ca *versus* Mg for the sampled carbonates (Figure 11) indicates that they mostly fall in a compositional range from calcite to dolomite (with some intermixed non-carbonate material). Two samples are very Mg-rich suggesting the presence of magnesite or intermixed non-carbonate material with a high Mg content.

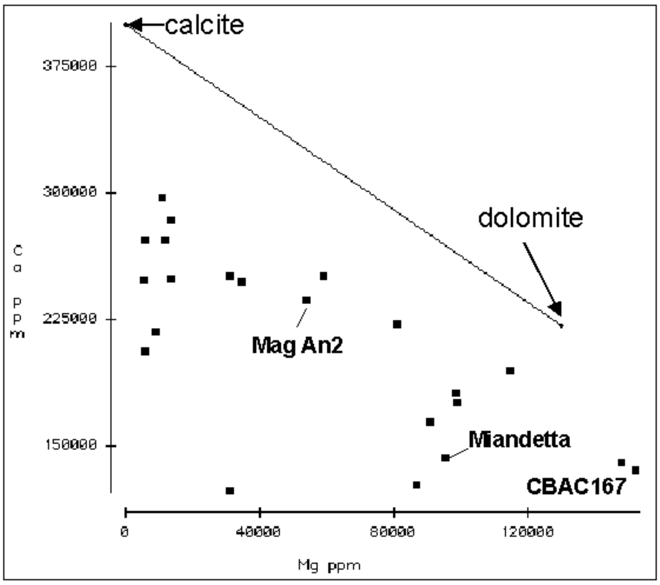

Figure 11. Plot of Ca versus Mg for calcrete samples from the Hermidale area. Diagonal line shows the compositional range between pure calcite and dolomite.

5 CONCLUSIONS

5.1 Regolith Architecture

The following conclusion points give insights into the regolith architecture of the Hermidale area, and so provide a framework for interpreting geochemical results:

- Colluvial sediments cover much of the area. Colluvial regolith-landform units are dominant in areas of higher elevation and relief, particularly in the southwestern part of the area. They are associated with north-northwest trending bedrock features. Alluvial plain units are dominant in the central-north and eastern parts.
- A ubiquitous layer of silt coats all landforms. More work is required to fully establish its aeolian origin.
- Drill holes should be spaced no more than 1 km apart to facilitate interpolation of regolith material units between drill holes.
- Ideally, drill holes through palaeochannel sediments should be sampled at 1 m intervals to facilitate adequate facies interpretation.
- Sediment materials are commonly composite, though some sediment units dominantly comprise a single sediment material with minor (<15%) other materials.
- The variable depth of sediments, both in palaeovalleys in the erosional domain in the west and beneath depositional plains in the east, indicates a palaeorelief greater than the present relief.
- Facies interpretation is necessary to determine if the change from regolith units with brown clays to those with grey clays could represent a change in depositional environment or weathering associated with a palaeoredox front due to a higher palaeowater table.
- The present water table ranges from 33 to 67 m in depth and intersects the saprolith below the base of sediments in all drill holes that encountered the water table.
- Gravel/sand units are common at the base of the oxidised zone above the reduced zone.
- Two general mineral assemblages are dominant within the transported and *in situ* regolith. The transported regolith shows a kaolinite ± illite ± smectite mineral assemblage, whereas the saprolite shows a kaolinite ± muscovite/phengite ± illite ±smectite mineral assemblage.
- Palynology indicates the reduced sediments are most likely to be Late Miocene to Early Pliocene. This correlates with the Lachlan Formation from palaeovalleys associated with the Lachlan River system, as well as correlatives in the Macquarie River system to the south-east.
- Magnetic sediments are mainly associated with palaeodrainage lines, which trends in similar directions to present drainage lines.
- Palaeosediments are more extensive than the obvious extent of magnetic sediments depicted on the 1.5VD magnetic imagery.
- Dominant bedrock lithologies are phyllite/siltstone, sandy phyllite and sandstone, and minor volcanics, chert and black shale.
- Highly weathered bedrock extends to at least 82 m depth.
- Vein quartz is common within saprolite.
- Silicification of saprolite is more common than ferruginisation, but is not widespread.
- Carbonates are common and are associated with the transported/saprolite interface or sediments higher in the profile.

5.2 Geochemistry

The following comments can be made about analytical and sampling procedures and the regolith geochemistry from the Hermidale area:

- The change in drilling procedure (*i.e.* purging the vacuum chamber by drilling 2 m of local material and discarding before re-starting drilling at a particular site: see Section 2.2) has avoided cross-hole contamination seen during the initial Sussex phase of drilling (Chan *et al*., 2001).
- The sampling and analytical methods employed give acceptable levels of precision and accuracy for this type of study, for most major and trace elements (see below and Appendix 8 for exceptions).

- Caution is advised when interpreting geochemical results for some elements analysed using multi acid dissolution methods, (*e.g.,* high Cr identifies mafic dykes but the absence of Cr does not preclude material from being mafic). Specifically, Ba, Cr, Ti and Zr values determined by ICP analysis should be regarded as minimum values because of the possibility of incomplete dissolution.
- K results are also affected by the analytical procedure (lower values for ICP than XRF, see Appendix 8) and so should also be used cautiously.
- PIMA shows changes down profiles and when integrated with geochemistry can help interpret materials encountered during drilling. Specifically, samples for which the TSA algorithm identifies only one mineral or does not identify any mineral phases should be checked to determine whether such material is mafic. In other profiles the coincidence of the mineralogical change from dominant mica to kaolinite coincides with loss of mobile elements like Zn.
- Gold is elevated in some surface and near surface samples and there is a high probability that such Au is associated with secondary regolith carbonate, “calcrete”.
- Mafic dykes occur in the rocks to the north and east of the Babinda Volcanics. Such dykes can be enriched in chalcophile elements such as Co, Cu and Zn.
- Anomalous Zn occurs in the Babinda Volcanics regionally (Fleming and Hicks, 2002). This study indicates that other mineralisation-associated elements may be present in Zn-rich profiles, possibly analogous to the Mt Windsor Volcanics (in which stratiform mineralisation generally occurs at a particular level in acid to intermediate volcanic sequences: Berry et al., 1992).
- Weak Au-As mineralisation occurs in CBAC 142, along strike from the Muriel Tank mineralisation.
- Weak As-Sb-Mo-W-Zn-(Cu)-(Au) mineralisation occurs in CBAC 167 and probably reflects the edge of more Pb-rich mineralisation (as found in nearby mine dump material).
- To gain the most useful geochemical information, an integrated approach using geochemical and mineralogical analysis (PIMA and XRD*)* is needed.

ACKNOWLEDGEMENTS

Eric Monteil (Geoscience Australia) undertook palynological investigations on selected sediment samples. Preparation of these samples was carried out in the palynological laboratory in Geoscience Australia. Susan Tate (ANU) determined the EC and pH for soil samples. Tin Tin Win (CSIRO) ran the XRD traces. Peter Milligan (Geoscience Australia) produced scaled topographic profiles from the Cobar regional digital elevation model for both the Hermidale and Sussex-Coolabah project areas, and guided aspects of geophysical image processing. Paul Wilkes (CRC LEME/Curtin University) processed geophysical images to facilitate mapping and fieldwork. Airborne geophysical data (DEM, gamma spectroradiometrics and magnetics) were supplied by the NSW Department of Mineral Resources. Anne Gibson (University of Canberra) entered data into Geoscience Australia databases and assisted with laboratory analyses. Simon Debenham (Geoscience Australia) assisted drilling operations by sampling and logging regolith cuttings. Paul Ferguson and Inga Zeilinger (Geoscience Australia) guided the use, respectively, of Geolog and Deviant software. Bill Pappas (Geoscience Australia) did the XRF on bottom hole drill samples. Algis Juodvalkis (CRC LEME/Geoscience Australia) guided the PIMA analysis. Tan Kok Piang (Geoscience Australia) provided helpful advice on aspects of the PIMA and XRD interpretations. Murray Woods (Geoscience Australia) digitally captured map coverage data, and Kylie Foster (CRC LEME/Geoscience Australia) guided the GIS map production. Jim Mason (Geoscience Australia) facilitated the printing of this report. Mike Craig (Geoscience Australia) provided editorial comment on the final draft of the report. All this assistance is acknowledged with appreciation.

REFERENCES

Berry, R.F., Huston, D.L., Stolz, A.J., Hill, A.P., Beams, S.D., Kuronen, U. and Taube, A., 1992. Stratigraphy, structure and volcanic-hosted mineralization of the Mount Windsor Subprovince, North Queensland, Australia. Economic Geology 87: 739-763.

Bureau of Meteorology, 2002. http://www.bom.gov.au/

Byrnes, J.G., 1993. Bourke 1:250 000 Metallogenic Map SH/55-10. Metallogenic Study and Mineral Deposit Data Sheets. 127 pp. Geological Survey of New South Wales, Sydney.

Chan R.A., Greene R.S.B., de Souza Kovacs N., Maly B.E.R., McQueen K.G. and Scott K.M., 2001. Regolith, geomorphology, geochemistry and mineralisation of the Sussex-Coolabah area in the Cobar-Girilambone region, north-western Lachlan Foldbelt, NSW. CRC LEME Report 166.

Fleming G. and Hicks M., 2002. Second programme of shallow reconnaissance aircore drilling, Hermidale area, Cobar NSW: interim report, GS2002/018. NSW Department of Mineral Resources.

Gilligan L.B. and Byrnes J.G., 1995. Cobar Metallogenic Map 1:250 000, Metallogenic Study and Mineral Data Sheets. Gilligan, L.B. and Byrnes, J.G., 1995. Cobar Metallogenic Map 1:250 000 SH/55-14.Metallogenic Study and Mineral Deposit Data Sheets. 240 pp. Geological Survey of New South Wales, Sydney.

Golden Cross Resources Ltd, 2000. Pipeline/Canbelego. Annual Report, 2000, p.16.

Helix Resources NL, 1988. Technical Report 2047, GS1988/223

Hill, S.M., McQueen, K.G. and Foster, K.A., 1999. Regolith carbonate accumulations in Western and Central NSW: characteristics and potential as an exploration sampling medilum. In Taylor, G.M., Pain, C.F. (Eds). State of the Regolith. Proceedings of Regolith 98, pp.191-208.

Jaquet, J.B. 1923. Report by Chief Inspector of Mines upon the Muriel Tank Goldfield. Department of Mines New South Wales Annual Report for 1922, 49-50.

Lintern, M.J. and Butt, C.R.M., 1998. Gold exploration using pedogenic carbonate (calcrete) Geological Society of Australia Special Publication 20, 200-208.

McQueen, K.G., Hill, S.M. and Foster, K.A., 1999. The nature and distribution of regolith carbonate accumulations in southeastern Australia and their potential as a sampling medium in geochemical exploration. Journal of Geochemical Exploration, 67, 67-82.

Pain, C.F., Chan, R.A., Craig, M.A., Gibson, D.L., Kilgour, P. and Wilford, J.R., 2002. RTMAP regolith database: field hand book users guide. Second Edition. CRC LEME Report 138

Placer Exploration Ltd., 1991. Annual and Final Report EL 3512 Nymagee, GS1991/071

Pan Australian Mining Ltd., 1986. Exploration Report EL 2339 Harts Tank area, GS1986/262

Planet Resources Group NL, 1988. Final Exploration Report EL3080 Hermidale, GS1988/294

Scott, K.M., 1988. Phyllosilicate and rutile compositions as indicators of Sn specialization in some southeastern Australian granites. Mineralium Deposita 23: 159-165.

Suppel, D.W. and Gilligan, L.B., 1993. Nymagee Metallogenic Map 1:250 000 SI/55-2: Metallogenic Study and Mineral Deposit Data Sheets. 171 pp. Geological Survey of New South Wales, Sydney.

Williamson W.H., 1986. Investigation of the groundwater resources of the Lachlan Valley alluvium. Part 1: Cowra to Jemalong Weir. Water Resources Commission. Hydrological Report No. 1986/12.

APPENDIX 1: DRILL HOLES NUMBERS AND SAMPLE INTERVALS

Field ID	GA site ID	Sample Interval (m)
CBAC139	2001700139	Surface – 41m
CBAC140	2001700140	Surface – 41m
CBAC141	2001700141	Surface – 33m
CBAC142	2001700142	Surface – 49m
CBAC143	2001700143	Surface – 63m
CBAC144	2001700144	Surface – 69m
CBAC145	2001700145	Surface – 69m
CBAC146	2001700146	Surface – 69m
CBAC147	2001700147	Surface – 69m
CBAC148	2001700148	Surface – 57m
CBAC149	2001700149	Surface – 69m
CBAC150	2001700150	Surface – 69m
CBAC151	2001700151	Surface – 17m
CBAC152	2001700152	Surface – 39m
CBAC153	2001700153	Surface – 17m
CBAC154	2001700154	Surface – 81m
CBAC155	2001700155	Surface – 61m
CBAC156	2001700156	Surface – 53m
CBAC157	2001700157	Surface – 29m
CBAC158	2001700158	Surface – 41m
CBAC159	2001700159	Surface – 29m
CBAC160	2001700160	Surface – 73m
CBAC161	2001700161	Surface – 49m
CBAC162	2001700162	Surface – 29m
CBAC163	2001700163	Surface – 45m
CBAC164	2001700164	Surface – 69m
CBAC165	2001700165	Surface – 13m
CBAC166	2001700166	Surface – 25m
CBAC167	2001700167	Surface – 21m
CBAC168	2001700168	Surface – 61m
CBAC169	2001700169	Surface – 33m
CBAC170	2001700170	Surface – 4m
CBAC171	2001700171	Surface – 57m
CBAC172	2001700172	Surface – 41m
CBAC173	2001700173	Surface – 41m
CBAC174	2001700174	Surface – 49m
CBAC175	2001700175	Surface – 37m
CBAC176	2001700176	Surface – 45m
CBAC177	2001700177	Surface – 33m
CBAC178	2001700178	Surface – 41m
CBAC179	2001700179	Surface – 41m
CBAC180	2001700180	Surface – 37m
CBAC181	2001700181	Surface – 53 m
CBAC182	2001700182	Surface – 61m
CBAC183	2001700183	Surface – 53m
CBAC184	2001700184	Surface – 49m
CBAC185	2001700185	Surface – 61m
CBAC186	2001700186	Surface – 41m
CBAC187	2001700187	Surface – 37m

APPENDIX 2: REGOLITH-LANDFORM MAPPING UNITS AND DESCRIPTIONS

Regolith-landform Unit	Description
ACar1	Alluvial channels with rounded to sub-angular sands, silts, clay and gravels, composed of quartz and lithic fragments within ephemeral meandering channels. Shows a high radiometric response in all channels indicating an acid volcanic provenance from the west.
ACar2	Alluvial channels with rounded to sub-angular sands, silts, clay and gravels, composed of quartz and lithic fragments within ephemeral meandering channels. Shows a potassium-dominated radiometric response indicating a granitic provenance from the south
Aap1	Alluvial plains with sub-rounded to sub-angular sands, silts and gravels, composed of quartz and lithic fragments, in low relief areas. Surface material consists of quartzose and lithic sand and gravel. Shows a high radiometric response in all channels indicating an acid volcanic provenance from the west.
Aap2	Alluvial plains with sub-rounded to sub-angular sands, silts and gravels, composed of quartz and lithic fragments, in low relief areas. Surface material consists of quartzose and lithic sand and gravel. Shows a mixed radiometric response from a provenance with granitic and acid volcanic rocks.
Aap3	Alluvial plains with sub-rounded to sub-angular sands, silts and gravels, composed of quartz and lithic fragments, in low relief areas. Surface material consists of quartzose and lithic sand and gravel. Shows a potassium-dominated radiometric response indicating a granitic provenance from the south.
Apd1	Depositional plains with sub-rounded to angular quartz and lithic sands, silts and minor gravels within low relief areas. Surface material consists of fine lithic and quartz sand and gravel. Shows a low radiometric response in all channels
Apd2	Depositional plains with sub-rounded to angular quartz and lithic sands, silts and minor gravels within low relief areas. Surface material consists of fine lithic and quartz sand and gravel. Shows a potassium-dominated, low radiometric response.
Afa1	Alluvial fan (gradient <1m/km) with sub-rounded to angular quartzose and lithic sands, silts and minor gravels within very low relief areas. Surface material consists of fine-grained lithic and quartz sand and gravel. Shows a potassium-dominated radiometric response indicating a dominant granitic provenance
Aed1	Erosional depressions with sub-rounded to sub-angular quartz and lithic sands, silt and clay and occasional gravels within depressions containing minor channels. Surface material consists of quartz sand and gravel and occasional maghemite.
CHpd1	Depositional plains with sub-rounded to sub-angular lithic and quartz sands and gravels within low relief areas. Surface materials consist of fine lithic and quartz sand and gravel with occasional maghemite and red-brown material.
CHpd2	Depositional plains with sub-rounded to sub-angular lithic and quartz sands and gravels within low relief areas. Surface materials consist of fine lithic and quartz sand and gravel with occasional maghemite and red-brown material. Shows a thorium-dominated radiometric response indicating ferruginous regolith material.
CHep1	Erosional plains with sub-angular to sub-rounded lithic and quartz sands and gravels within low relief areas. Surface materials consist of fine to medium lithic and quartz sand and gravel with occasional maghemite and red-brown material.
CHep2	Erosional plains with sub-angular to sub-rounded lithic and quartz sands and gravels within low relief areas. Surface materials consist of fine to medium lithic and quartz sand and gravel with occasional maghemite and red-brown material. Shows a thorium-dominated radiometric response indicating ferruginous regolith material.
CHer1	Rises with angular to sub-rounded lithic and quartz sands and gravels mantling and flanking areas with moderate relief. Surface materials consist of coarse lithic and quartz sand and gravel lags with occasional maghemite and red-brown material.

APPENDIX 2 (continued)

SSep1	Erosional plains with exposures of slightly (to moderately) weathered saprolite in areas of low topographic relief. Surface materials consist of sub-angular to sub-rounded lithic and quartz sands and lags with red-brown material.
SSer1	Rises with exposures of slightly (to moderately) weathered saprolite in areas of slight topographic relief. Surface materials consist of angular to sub-rounded lithic and quartz sands and lags with red-brown material.
SSel1	Low hills with exposures of slightly (to moderately) weathered saprolite in areas of moderate topographic relief. Surface materials consist of angular to sub-angular lithic and quartz sands and lags with red-brown material.

APPENDIX 3: DEPTH OF TRANSPORTED MATERIAL AND WATER TABLE FOR DRILL HOLES

Hole Number	Depth of Transported (m)	Water Table (m)	Total Depth (m)
CBAC139	1		43
CBAC140	1	41	43
CBAC141	1		33
CBAC142	1		47.5
CBAC143	5		61.5
CBAC144	1		69
CBAC145	2		69
CBAC146	19	65	69
CBAC147	2		69
CBAC148	11		57
CBAC149	1		69
CBAC150	4	60	69
CBAC151	1		18
CBAC152	35		37.5
CBAC153	>16		16
CBAC154	11	60	82
CBAC155	13		60
CBAC156	7		53
CBAC157	19		30
CBAC158	>42	36	42
CBAC159	1.5		31
CBAC160	13	67	75
CBAC161	8		47.5
CBAC162	2		30
CBAC163	3		45
CBAC164	1		69
CBAC165	3		12.5
CBAC166	2		27
CBAC167	1		21
CBAC168	3		63
CBAC169	3		34
CBAC170	1		6
CBAC171	7		57
CBAC172	1		43
CBAC173	2	33	41
CBAC174	3		49
CBAC175	1		37
CBAC176	2		45
CBAC177	1		33
CBAC178	1		43
CBAC179	15		41
CBAC180	3		39
CBAC181	31	43	53
CBAC182	19	58	61
CBAC183	35	45	54
CBAC184	31	46	51
CBAC185	9	48	60
CBAC186	15	38	42
CBAC187	35	34	36

APPENDIX 4: ACID ATTACK ON DRILL HOLE SAMPLES

(**M** – major carbonate reaction, **m** – minor carbonate reaction, ____ represents position of unconformity between soil/transported and *in situ* regolith)

CBAC	139	140	141	142	143	144	145	146	147	148	149	150
0m		**m**				**m**	**m**		**m**			
0-1m	**M**___	**m**____	**M**____	_____		**m**____	**M**		**m**		_____	**m**
1-2m	**m**	**m**	**M**	**m**			_____		**m**____		**m**	**m**
2-3m				**M**			**M**		**M**	**M**	**M**	**m**
3-4m				**m**			**M**				**m**	_____
4-5m			**M**		_____						**m**	**M**
5-6m			**M**		**M**			**m**				**M**
6-7m					**M**					**m**		**m**
7-8m		**M**			**m**				**m**			**m**
8-9m			**m**									**M**
9-11m										_____		**m**
11-13m												**m**
13-15m												
15-17m		**M**										
17-19m								_____				
19-21m												
21-23m												
23-25m												
25-27m												
27-29m												
29-31m												
33-35m												
35-37m												
37-39m												
39-41m												
41-43m												
43-45m												
45-47m												
47-49m												
49-51m												
51-53m												
53-55m												
55-57m												
57-59m												
59-61m												
61-63m												

APPENDIX 4 (continued)

CBAC.	151	152	153	154	155	156	157	158	159	160	161	162
0m			**m**	**m**					**m**			**m**
0-1m	**m**____		**m**	**m**				**M**	**m**____		**m**	**m**
1-2m	**m**	**m**	**m**	**m**	**m**	**M**	**M**		**M**	**m**	**M**	**m**____
2-3m	**m**	**M**	**m**	**m**		**M**	**M**		**M**		**M**	**m**
3-4m	**m**	**m**				**M**	**m**		**M**			**m**
4-5m	**m**	**m**	**m**		**m**	**M**	**m**		**m**	**M**	**m**	**m**
5-6m	**m**	**m**			**m**	**M**	**m**	**M**	**M**	**M**		**m**
6-7m	**m**	**m**			**m**	**M**____	**m**		**m**	**M**		**m**
7-8m	**m**	**m**	**M**			**M**				**m**	**m**____	**m**
8-9m	**m**	**m**	**M**		**m**	**M**				**m**	**m**	
9-11m	**m**			**m**____	**m**						**m**	**m**
11-13m	**m**			**m**	**m**____					______		
13-15m	**m**			**m**						**m**		
15-17m	**m**											
17-19m	**m**						______					
19-21m												
21-23m												
23-25m												
25-27m												
27-29m												
29-31m												
33-35m		______										
35-37m												
37-39m												
39-41m												
41-43m												
43-45m												
45-47m												
47-49m												
49-51m					**m**							
51-53m					**m**							
53-55m												
55-57m					**m**							
57-59m												
59-61m					**m**							
61-63m												

APPENDIX 4 (continued)

CBAC.	163	164	165	166	167	168	169	170	171	172	173	174
0m	**m**							**m**				
0-1m		______	**m**	**m**	**M____**	**M**	**m**	**m____**		**m____**	**m**	**m**
1-2m	**M**		**m**	**M____**	**m**	**M**	**M**		**M**	**m**	**m____**	**m**
2-3m	**M____**		______	**M**		**m____**	**m____**	**m**	**m**	**m**	**m**	______
3-4m	**M**						**m**	**m**	**m**	**m**	**m**	**m**
4-5m					**m**		**m**		**m**	**m**	**m**	
5-6m							**m**		**m**	**m**	**m**	**m**
6-7m					**m**	**m**			**m____**	**m**		
7-8m		**m**	**M**			**m**			**M**			
8-9m	**m**					**m**			**m**	**m**		
9-11m	**m**								**M**	**m**		
11-13m			**m**						**M**	**m**		
13-15m									**m**			
15-17m				**M**								
17-19m												
19-21m												
21-23m												
23-25m												
25-27m	**m**											
27-29m	**m**											
29-31m	**m**											
33-35m												
35-37m												
37-39m												
39-41m												
41-43m												
43-45m												
45-47m												
47-49m												
49-51m												
51-53m												
53-55m												
55-57m												
57-59m												
59-61m												
61-63m												

APPENDIX 4 (continued)

CBAC	175	176	177	178	179	180	181	182	183	184	185	186	187
0m						m							
0-1m	_____		_____	_____	m	m		m					
1-2m	m	m__		M	m		m	m		m	M		
2-3m	m	M		M	m	M____	m	m	M	m			m
3-4m		m				m		m		M	m		
4-5m	m	m								m			
5-6m	m					m			m				m
6-7m													m
7-8m	m									m	M		m
8-9m	m				m					m	_____	M	m
9-11m					m					m		M	
11-13m					m					m			
13-15m					_____							_____	
15-17m												m	
17-19m								_____				m	
19-21m													
21-23m													
23-25m													
25-27m													
27-29m													
29-31m							_____			_____			
33-35m									_____				_____
35-37m													
37-39m													
39-41m													
41-43m													
43-45m													
45-47m													
47-49m													
49-51m													
51-53m													
53-55m													
55-57m													
57-59m													
59-61m													
61-63m													

APPENDIX 5: FIELD LOGS OF REGOLITH MATERIAL INTERSECTED IN DRILL HOLES

See accompanying file.

APPENDIX 6: PIMA ANALYSIS LOGS

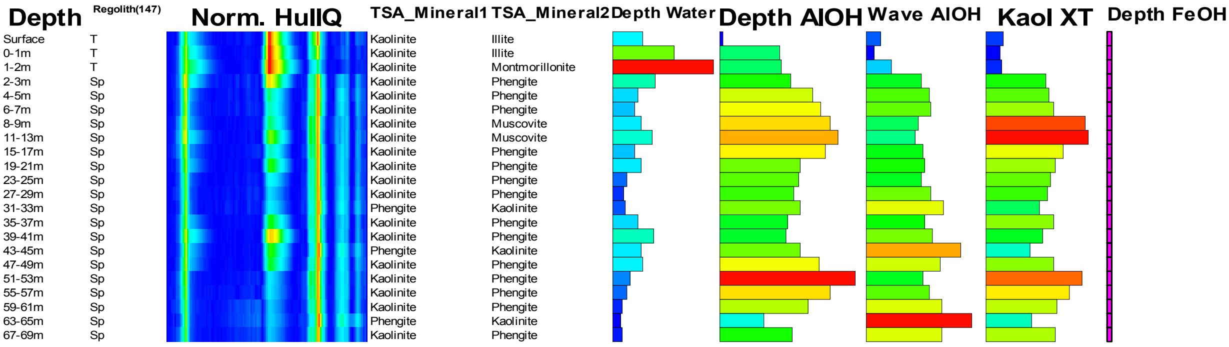

6A: PIMA analysis of the regolith profile of drill hole CBAC147. The unconformity between transported and *in situ* regolith lies at 2 m. The saprolitic mineral assemblage consists of kaolinite (dominant), phengite and muscovite.

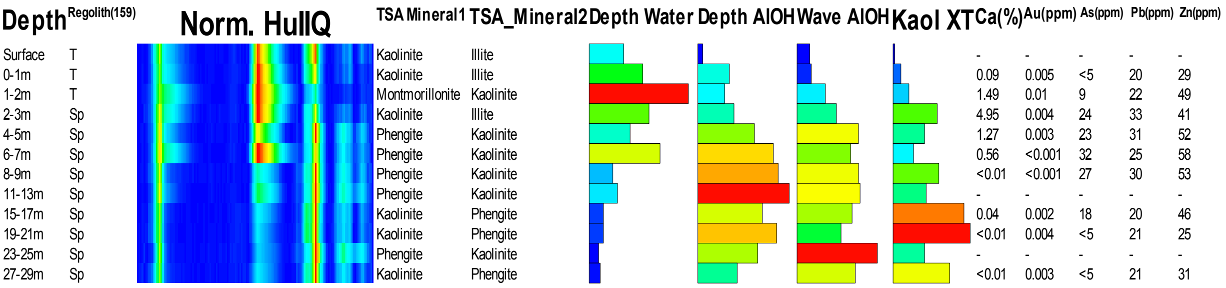

6B: PIMA analysis of the regolith profile of drill hole CBAC159. The transported-*in situ* unconformity lies at 35 m. The saprolitic mineral assemblage consists of kaolinite (dominant) and phengite.

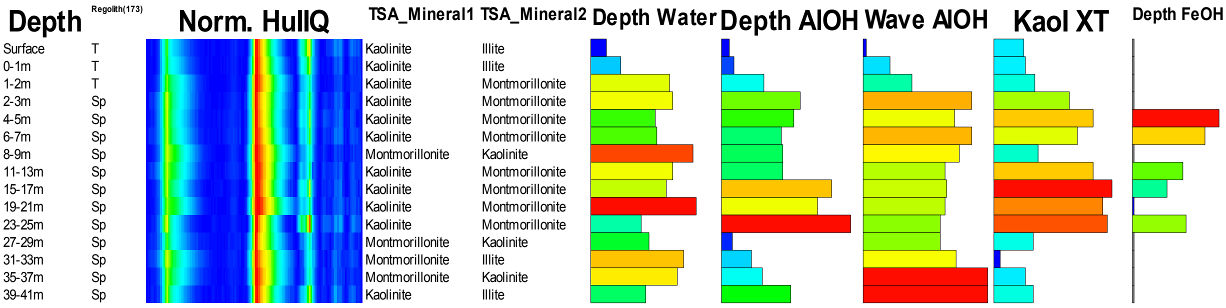

6C: PIMA analysis of the regolith profile of drill hole CBAC173. The transported-*in situ* unconformity lies at 2 m. The saprolitic mineral assemblage consists of kaolinite (dominant), muscovite and smectite.

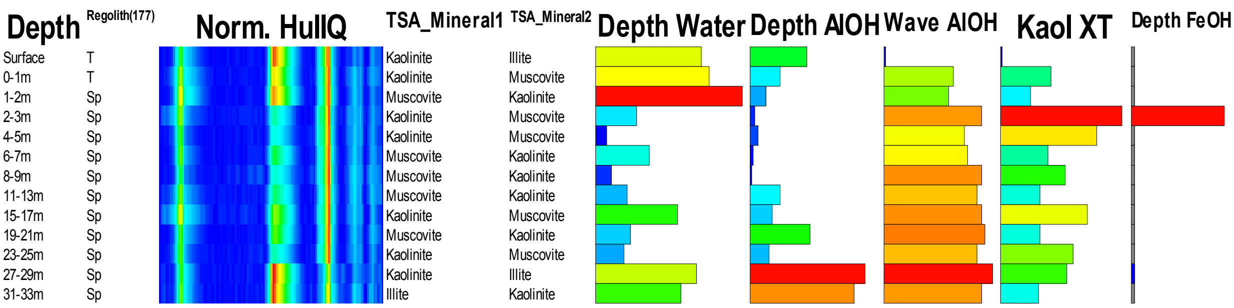

6D: PIMA analysis of the regolith profile of drill hole CBAC177. The transported-*in situ* unconformity lies at 1 m. The saprolitic mineral assemblage consists of kaolinite (dominant) muscovite and illite.

APPENDIX 6: PIMA ANALYSIS LOGS (continued)

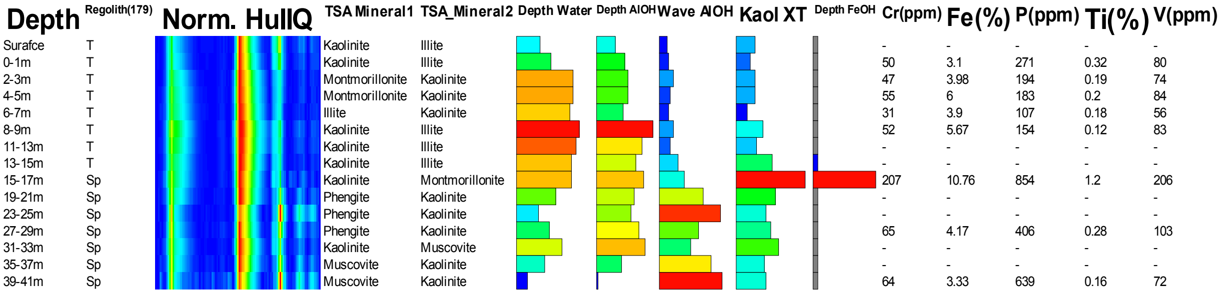

6E: PIMA analysis of the regolith profile of drill hole CBAC179. The transported-*in situ* unconformity lies at 15 m. In the 15-17m interval highly crystalline kaolinite dominate, and the deep FeOH absorption peak indicates that the saprolite is derived from the weathering of a mafic dyke.

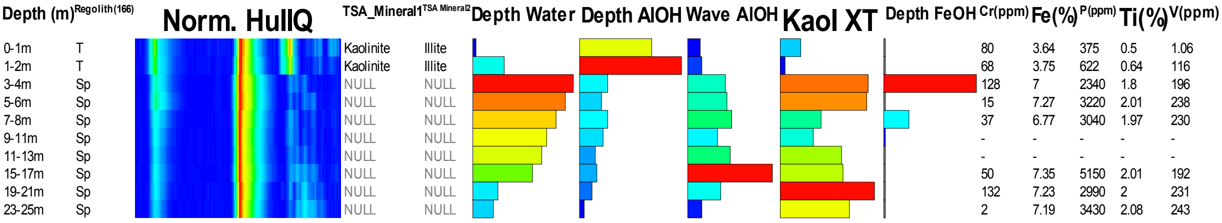

6F: PIMA analysis of the regolith profile of drill hole CBAC166. The transported-*in situ* unconformity lies at 2 m. The PIMA did not detect phyllosilicates in the saprolite giving Null values for the mineral identification. This profile is recognised as containing mafic material due to highly crystalline kaolinite and the geochemistry.

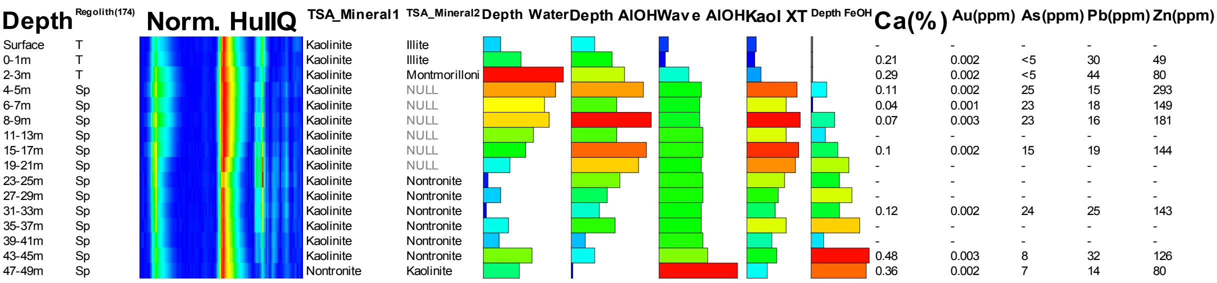

6G: PIMA analysis of the regolith profile of drill hole CBAC174. The transported-*in situ* unconformity lies at 3 m. The PIMA shows the highest FeOH absorption peaks within the saprolite for any hole within the Hermidale study area. This hole is also the most felsic of all holes drilled.

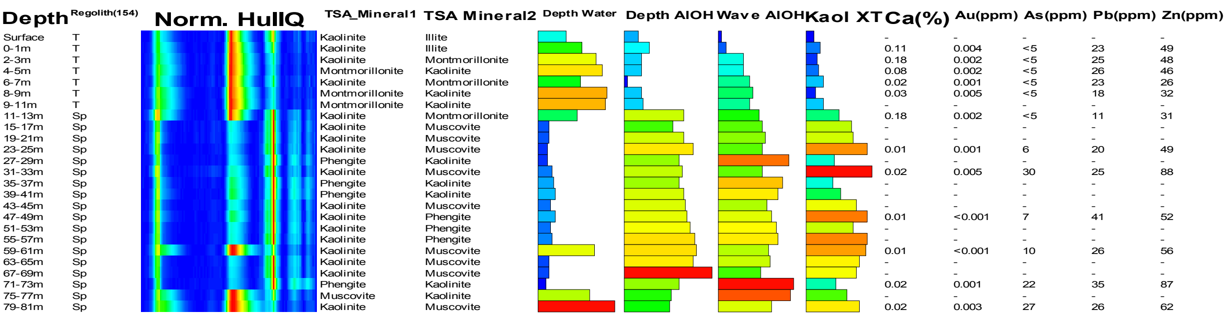

6H: PIMA analysis of the regolith profile of drill hole CBAC154. The transported-*in situ* unconformity lies at 11 m. The PIMA results show there is a clear boundary at the transported/saprolite unconformity. The unconformity is highlighted by a marked change in all algorithms used, particularly the depth to water and kaolinite crystallinity.

APPENDIX 6: PIMA ANALYSIS LOGS (continued)

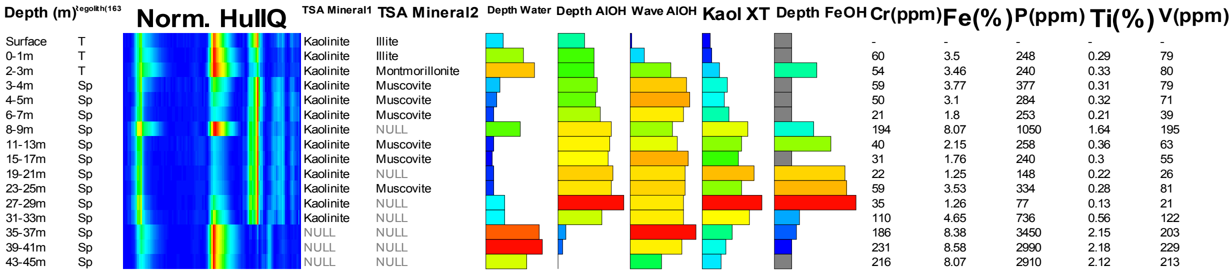

6I: PIMA analysis of the regolith profile of drill hole CBAC163. Elevated Ti, Fe, Mn, P, Sr and V at 8-9 m (upper saprolite) and 33-45 m (lower saprolite) indicate mafic dykes. These mafic intervals are characterised by low abundances of clay minerals.

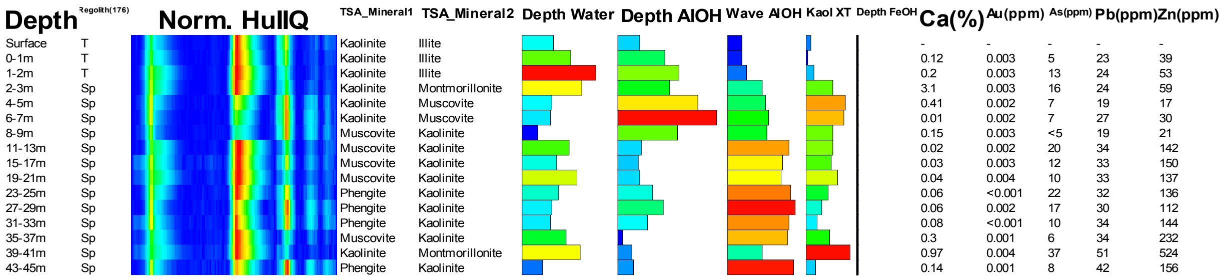

6J: PIMA analysis of the regolith profile of drill hole CBAC176. The mafic interval (39-41 m) does not contain elevated Cr but Fe, Ti, P and V are high (Appendix 10). The depth of the Al-OH feature (abundance of mica) is distinctly lower than shallower samples. Zinc is strongly enriched in the mafic interval and surrounding samples.

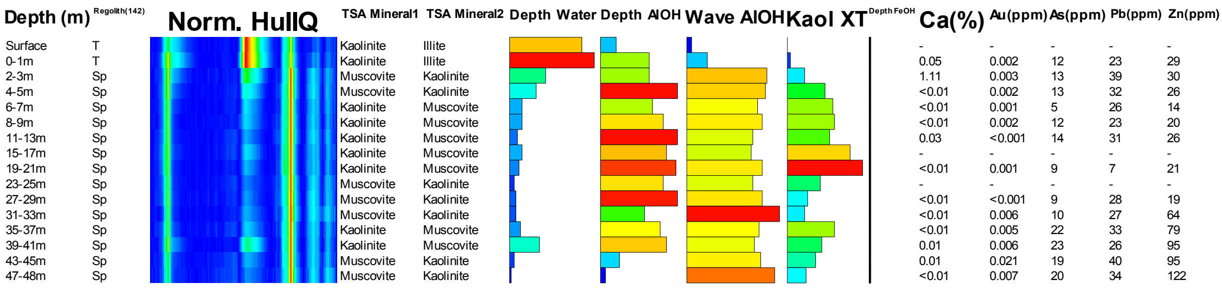

6K: PIMA analysis of the regolith profile of drill hole CBAC142. Gold is elevated below 29 m with As, Cu and Zn also elevated. Zinc is distinctly elevated below 39 m.

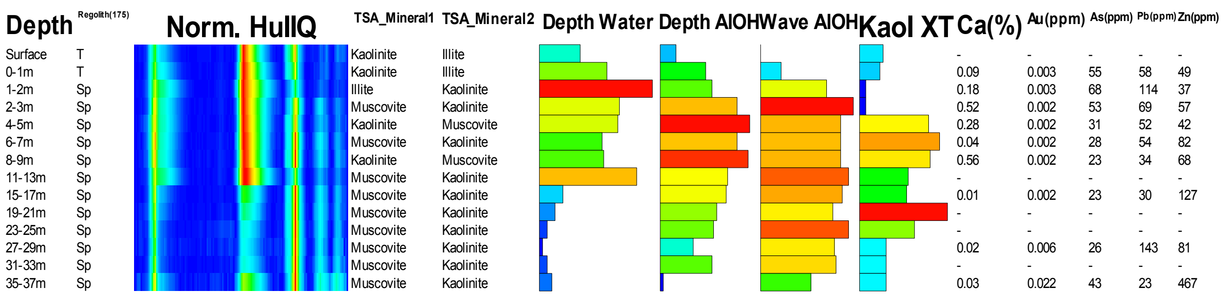

6L: PIMA analysis of the regolith profile of drill hole CBAC175. Arsenic is elevated throughout but Au is only anomalous below 25 m where it is sometimes associated with Pb and W. Highly anomalous W and Zn occur in the ferruginous basal sample.

APPENDIX 6: PIMA ANALYSIS LOGS (continued)

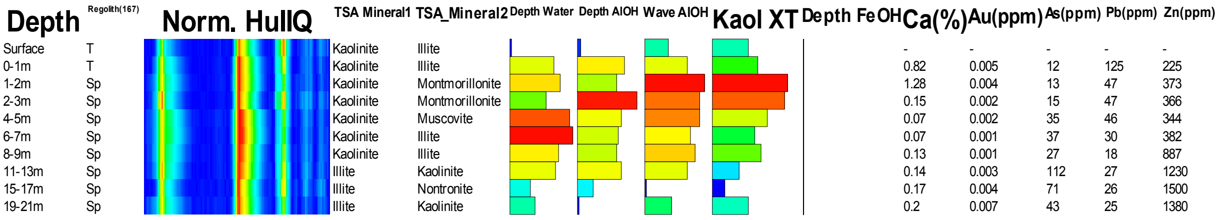

6M: PIMA analysis of the regolith profile of drill hole CBCA167. Substantial As, Sb, Cu, Mo, W and Zn occur throughout this hole through Babinda Volcanics. Zinc is particularly high in the basal sample, with values >700ppm up to 7 m.

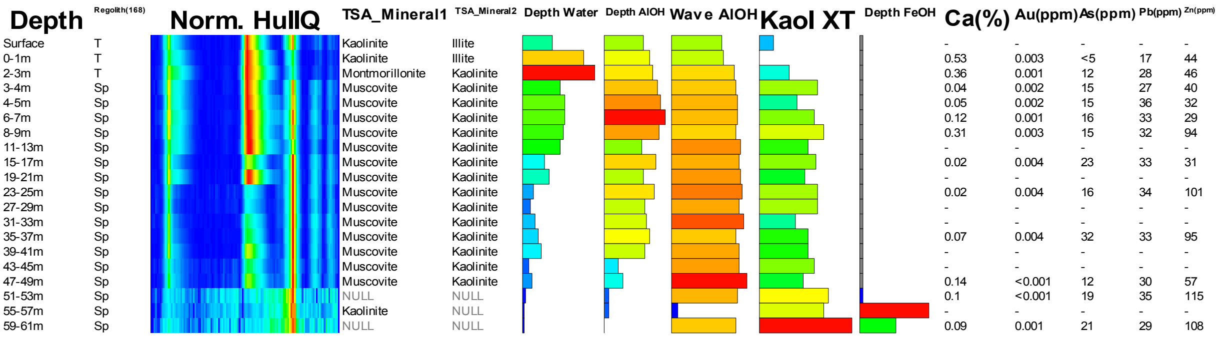

6N: PIMA analysis of the regolith profile of drill hole CBAC168. This hole passes into black carbonaceous shale with pyrite and chlorite below 47 m. The low Au and base metal contents of the shale interval suggest that the pyrite is barren.

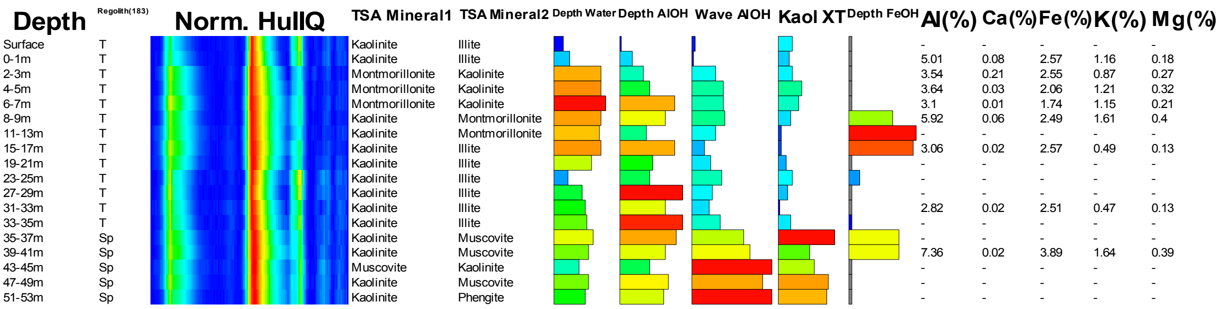

6O: PIMA analysis of the regolith profile of drill hole CBAC183. This profile through 35 m of transported material shows considerable variation within the different sediment types *e.g.* see the strong development of Fe-OH feature between 8and 17 m.

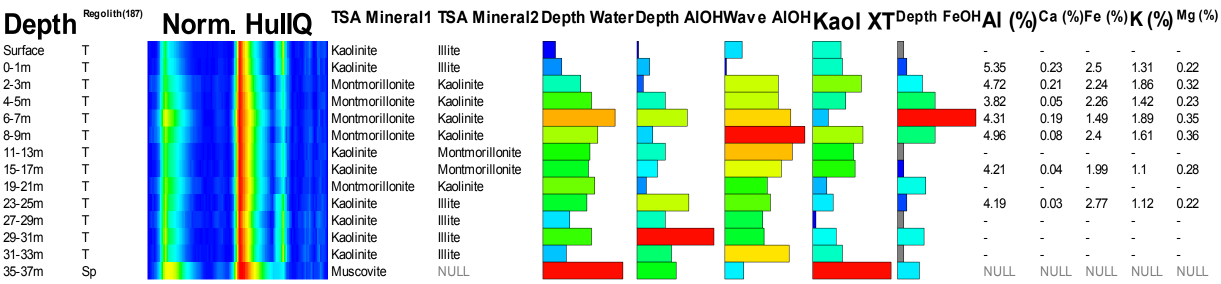

6P: PIMA analysis of the regolith profile of drill hole CBAC187. The Pima spectra for this profile through 36 m of transported material clearly shows the transition from transported to *in situ* regolith.

APPENDIX 7: PALYNOMORPHS IN GREY CLAYS USED FOR DATING SEDIMENTS

A. CBAC154, 2-4 m. *Malvacipollis subtili.*
B. CBAC182, 2-3 m. Pollen grain probably *Nothofagidites falcatus*
C. CBAC182 2-3 m. *Haloragacidites harrisii*
D. CBAC184, 8-9 m. *Cingulatisporites ?bifurcatus*
E. CBAC185, 8-9 m. *Chenopodipollis chenopodiaceoides*
F. CBAC184, 8-9 m. *Rudolphisporis rudolphi*

Palynology by Eric Monteil, Geoscience Australia
Scale bar is 25 micrometres

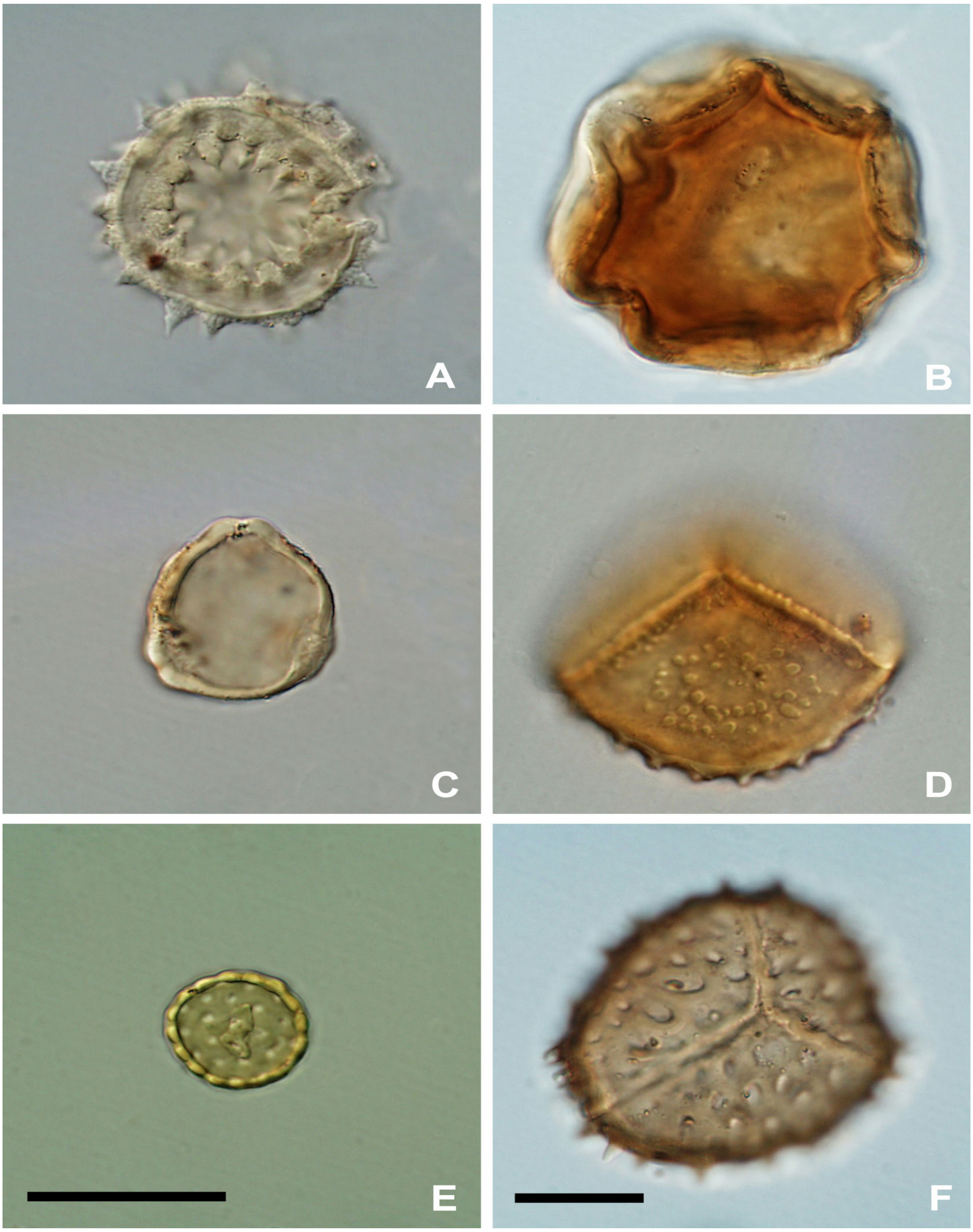

APPENDIX 8: GEOCHEMICAL DATA QUALITY AND RELIABILITY

A8-1. Analytical precision

As a test of analytical precision for the multi acid digest and ICP-MS and ICP-OES methods, replicate samples were taken from a carefully homogenised bulk sample from CBAC 150. A 15 kg sample from interval 31-33 m was homogenised by running the sample through a sample splitter, combining mixing and resplitting four times. Seven sub-samples of approximately 2 kg were prepared in this way and five were submitted for analysis. This process, combined with some degree of mixing of the sample by the air-core drilling technique should give a reasonably homogeneous sample, prior to milling and analysis. The results of the replicate analyses are presented in Fig. A8-1. They show that the multi acid digest approach was able to achieve very good precision for most elements except, Ti, Cr, and Zr (elements likely to be largely or partly hosted by resistate minerals), K (probably reflecting non-total digestion of muscovite or variable formation of potassium perchlorate during the digestion process used: see below), and to some extent Al (which is the most abundant element, with variability possibly reflecting imperfect homogenisation or dissolution of the sample). For most trace elements precision was good except for Pb and As. The replicate analyses for gold show values around 3-4 ppb, a little above the detection limit of 1 ppb. The results of the replicate analyses and standard deviations are shown in Table A8-1.

It should be noted that the dissolution procedure ME-ICP61, used by ALS-Orange to dissolve the rock powders involves the evaporation of the excess $HF/HClO_4/HNO_3$ acids only to near dryness to prevent the loss of volatile elements like As and Sb. However, this procedure does result in low recoveries of K and Rb (when the residue is redissolved) due to the formation of insoluble K and Rb perchlorates. Comparison of XRF-determined K with ICP-determined K in bottom-of-hole samples in these samples suggests that the latter may be underestimated by several percent, particularly in samples containing high abundances of mica. Thus the K contents reported in this report should be regarded as minimum values only and used cautiously.

A8-2 Laboratory precision and accuracy

A series of laboratory duplicates were analysed for 58 of the samples submitted to ALS-Chemex laboratories. Results of these duplicate determinations are presented in Appendix 10. A number of internal standards were also analysed by the laboratory for each of the 5 batches of samples submitted.

Table A8-1: Replicate analyses and standard deviations for samples from CBAC150 (31-33m).

Sample No.	Au (ppm)	Ag (ppm)	Al (%)	As (ppm)	Ba (ppm)	Be (ppm)	Bi (ppm)
CB1791	0.004	-0.5	11.16	12	824	4.3	4
CB1792	0.004	-0.5	11.46	11	833	4.7	-2
CB1793	0.002	-0.5	11.61	17	849	4.7	7
CB1794	0.002	-0.5	10.13	13	760	4.7	6
CB1795	0.002	-0.5	9.78	14	716	4.8	6
Stand dev	0.001	0.00	0.8	2.30	56	0.2	3.6

Sample No.	Ca (%)	Cd (ppm)	Co (ppm)	Cr (ppm)	Cu (ppm)	Fe (%)	K (%)
CB1791	0.01	-0.5	2	96	33	5.37	2.21
CB1792	0.01	-0.5	2	104	36	5.49	1.11
CB1793	0.01	-0.5	2	110	35	5.48	2.57
CB1794	-0.01	-0.5	2	114	35	5.23	1.98
CB1795	-0.01	-0.5	2	115	35	5.21	1.9
Stand dev	0.01	0.00	0.00	8	1	0.13	0.54

Sample No.	Mg (%)	Mn (ppm)	Mo (ppm)	Na (%)	Ni (ppm)	P (ppm)	Pb (ppm)
CB1791	0.52	67	-1	0.09	24	574	32
CB1792	0.52	70	-1	0.09	26	692	33
CB1793	0.53	70	1	0.09	26	667	32
CB1794	0.47	68	-1	0.09	25	647	28
CB1795	0.45	65	-1	0.09	25	645	26
Stand dev	0.04	2	0.00	0.00	0.8	44	3.0

Sample No.	S (%)	Sb (ppm)	Sr (ppm)	Ti (%)	V (ppm)	W (ppm)	Zn (ppm)
CB1791	-0.01	6	41	0.13	124	-10	84
CB1792	-0.01	-5	42	0.37	131	-10	86
CB1793	-0.01	-5	44	0.34	130	-10	86
CB1794	-0.01	9	35	0.27	132	-10	85
CB1795	-0.01	-5	34	0.31	131	-10	84
Stand dev	0.00	6.9	4.4	0.09	3	0.00	1.0

Sample No.	Zr (ppm)
CB1791	93
CB1792	105
CB1793	106
CB1794	102
CB1795	103
Stand dev	5

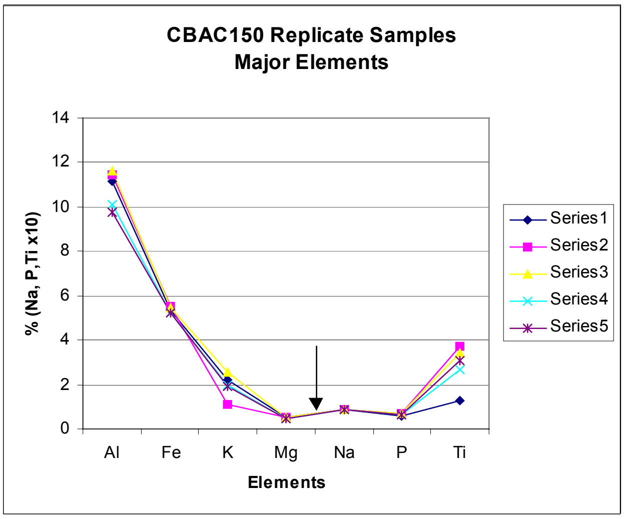

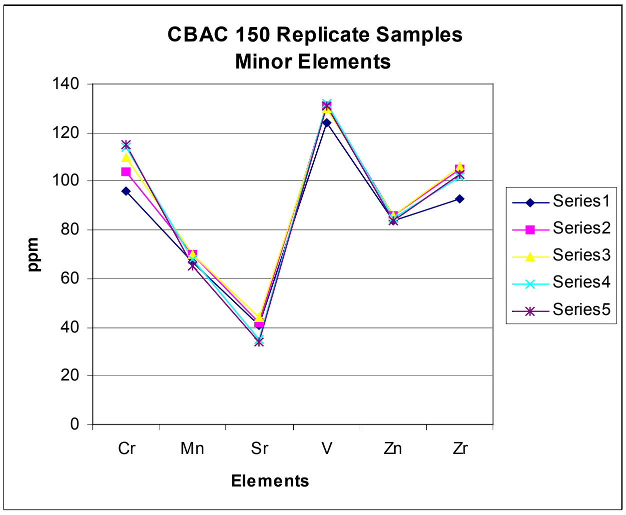

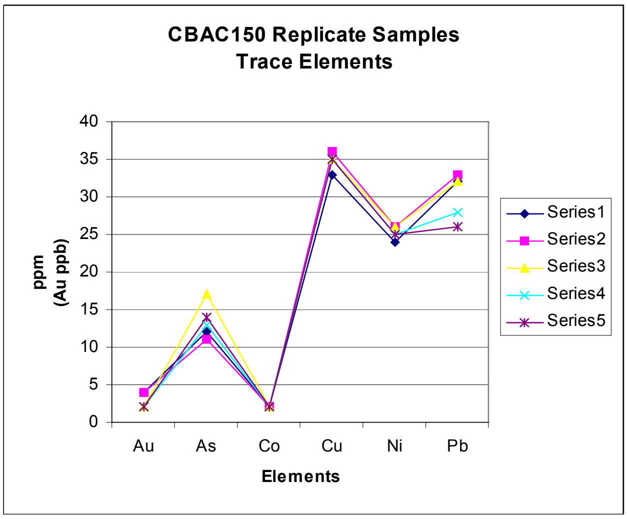

Figure A8-1. Plots showing results of replicate analyses of major, minor and trace elements for 5 sub-samples from CBAC150 32-33m.

A8-3 Sample Representativeness

To test the degree to which samples are representative of the bulk interval sampled by air core drilling, duplicate samples were collected from the same bulk samples. Most of the duplicates were collected from the bulk sample bags during a second stage of re-sampling, one month after the original sampling. Comparisons for major, minor and trace elements for five pairs of duplicates are presented in Figs A8-2, 3, 4. Most duplicates show good comparison, except for some elements including K, Ti, As, Bi, Be and Pb. Most of these elements showed variability in the replicate samples suggesting lower analytical precision. Gold in the duplicates compares well over the range 2-18 ppb. These results suggest that the bulk samples from the air core drilling technique are reasonably well homogenised and that 0.5 kg samples from these bulks are sufficiently representative of the interval drilled for the purpose of the exercise.

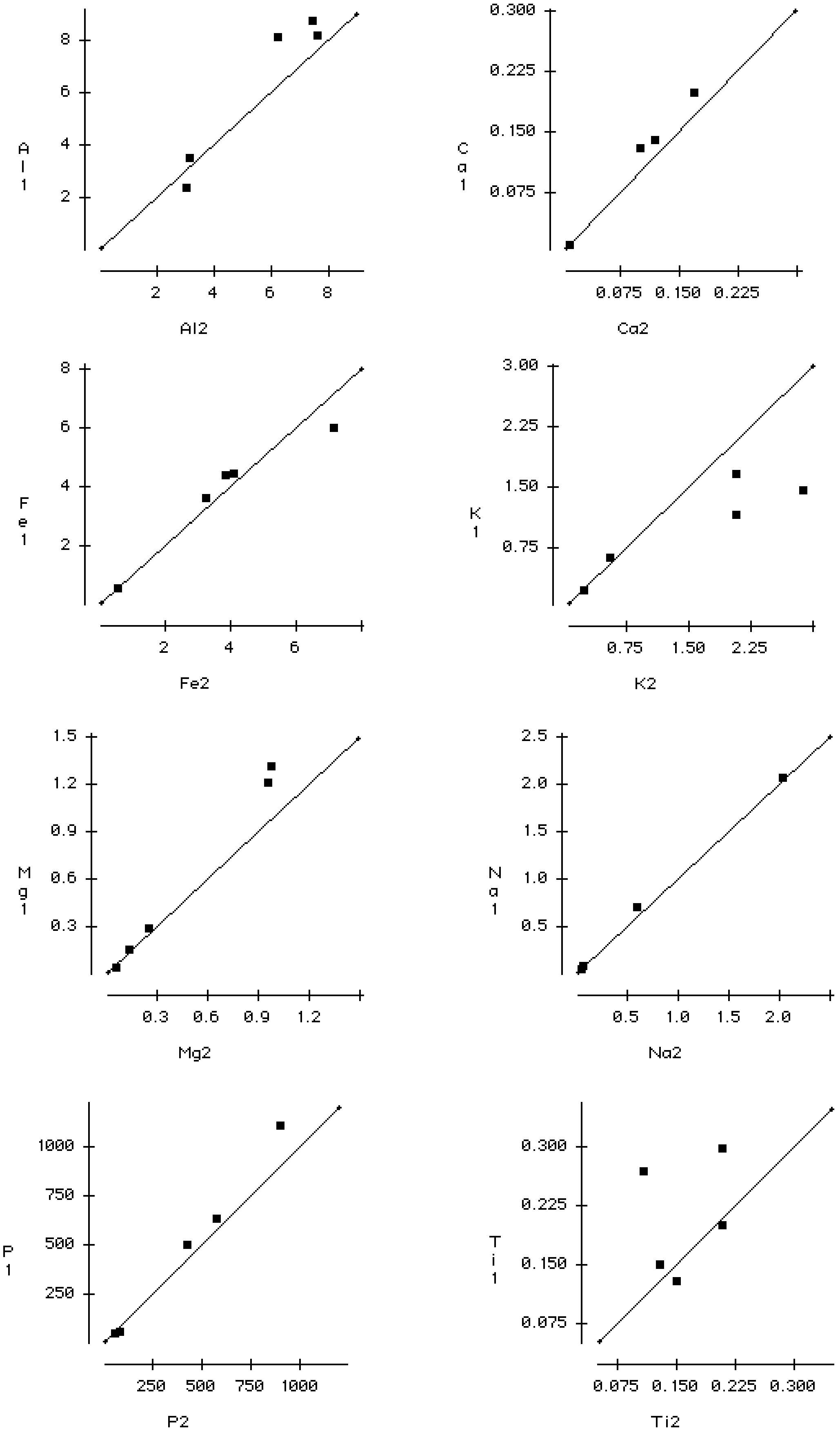

Figure. A8-2. Determinations of duplicate samples for Al, Ca, Fe, K, Mg, Na, Ti (%) and P (ppm).

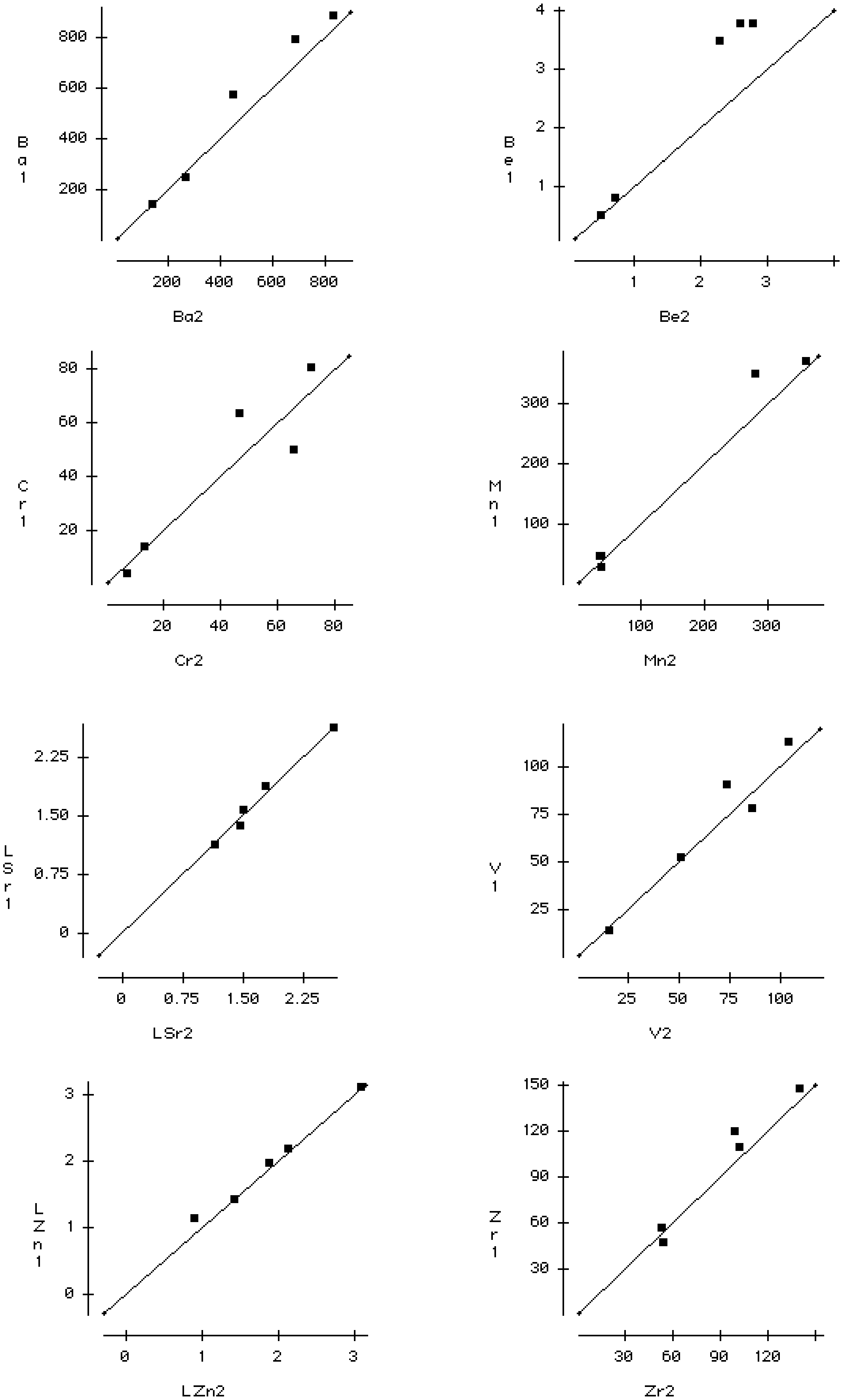

Figure A8-3. Determinations of duplicate samples for Ba, Be, Cr, Mn, log Sr, log Zn and Zr (ppm).

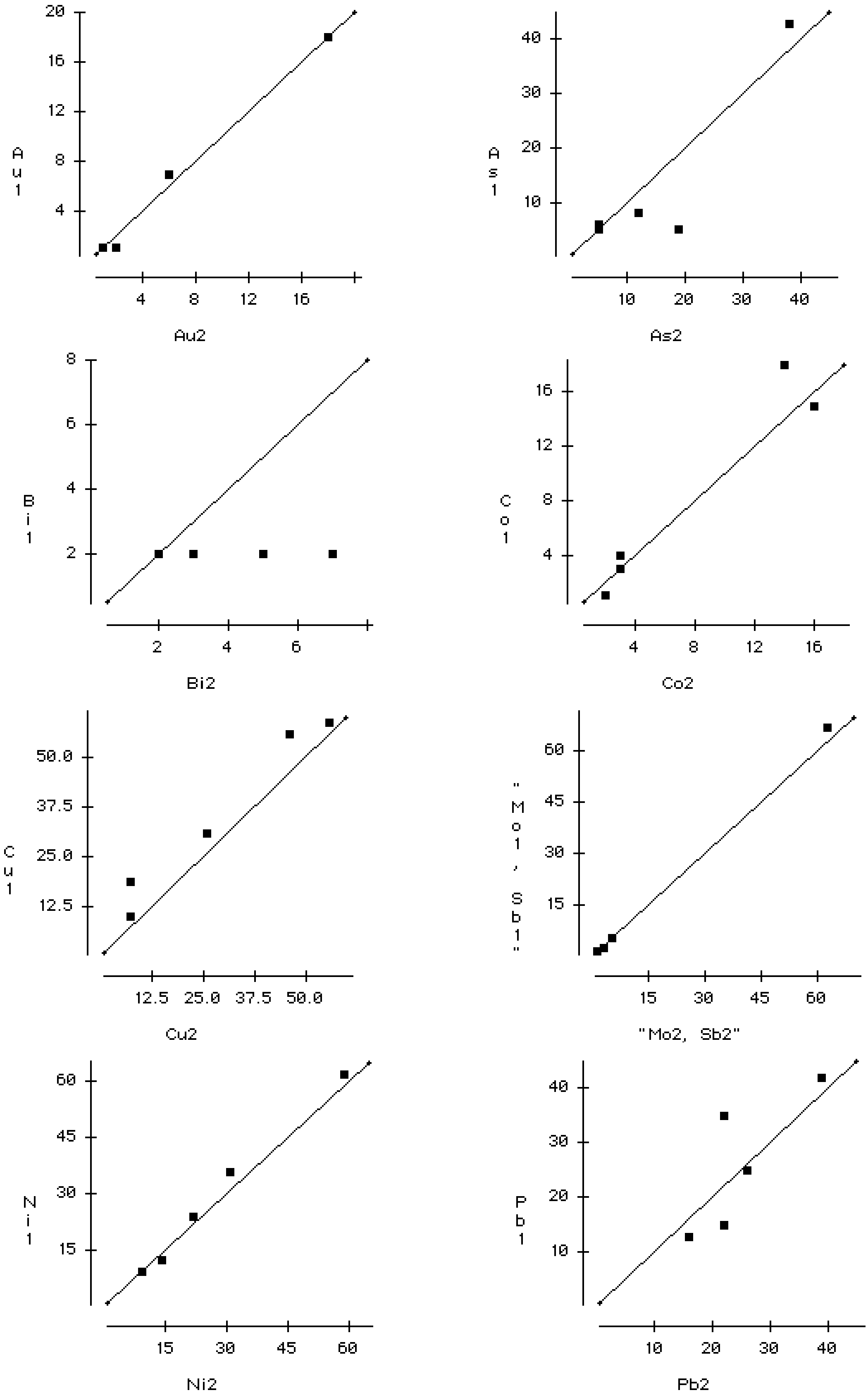

Figure A8-4. Determinations of duplicate samples for Au (ppb) As, Bi, Co, Ni, Pb (ppm).

APPENDIX 9: INVESTIGATION OF "REGOLEACH" ANALYSIS

The potential of the "Regoleach" partial leach technique was assessed as part of the geochemical study on the Hermidale project.

Composite samples of the first 1 m interval for each air core hole were subjected to "regoleach" analysis in addition to the normal acid digest procedure. A number of sites that returned anomalous "regoleach" results were checked by taking one or more soil samples at 20-30 cm depth around the drill hole collar (on a box or linear pattern, 50-100 m from the collar).

Results of the "Regoleach" assessment can be summarised as follows:

- In general the "Regoleach" results detected anomalies that were also found in deeper drilling. There were several examples where anomalous "Regoleach" values were not reflected deeper in the profile or where follow up "Regoleach" sampling did not reproduce the earlier result (particularly for Ag).

- Regoleach results appear to be highly dependant on the nature of the soil or near surface regolith and the depth of sampling. This is well illustrated by data from two sites.

The first site was in an area of known minor mineralisation with associated Pb-Zn-Bi-Mo-W-As and minor Cu-Au. Elevated levels of these elements were found down the profile of air core hole CBAC167. The site is at a very low rise in an erosional setting. The soil is a thin (<0.5 m) lithosol with largely *in situ* components.

The second site showed elevated levels of Cu, Au, Bi, Zn and Cu at depth in air core hole CBAC157. This site is on a depositional plain with a thicker (ca. 1 m) soil composed largely of transported components.

At the first site the "Regoleach" results were compared from a composite of the first metre of air core drilling and from soil samples collected at ca. 20 cm depth from four sites around the drill hole (at 100 m distance in four directions). All samples showed anomalous levels of As, Bi, Mo, Sb and W. Values were similar between the air core sample and some of the soil samples. Lead and Zn values were higher in the air core "regoleach" sample than all the soil samples.

At the second site "Regoleach" results were compared from the first metre of air core drilling and from soil samples collected at 20-30 cm depth from four sites at 50 and 100 m north and south of the drill hole. Values for As, Bi and Cu were significantly higher in the 1 m composite than in the near surface soil samples. The latter has possibly sampled some of the *in situ* part of the regolith profile.

These results indicate that in the case where the regolith is mostly *in situ*, "Regoleach" has been able to detect anomalies in a range of pathfinder elements, and in some cases (*e.g.* As and Bi) with better discrimination than bulk analysis (because of lower detection limits). Where the regolith is mostly transported material "Regoleach" has been much less successful.

Based on the Hermidale sheet study:

- "Regoleach" appears to be particularly useful for detecting As anomalies in *in situ* regolith and can give better discrimination than "total" digest analysis. It also appears to give useful results for Bi, Mo, Sb and W in this type of regolith.
- "Regoleach" values for Ag appear to be erratic.
- In this study Cu and Zn showed a much weaker signal in "Regoleach" than in the multi-acid technique. "Regoleach" Cu and Zn values were below background levels over mineralised sites.

APPENDIX 10: GEOCHEMICAL DATA FOR THE HERMIDALE AREA

See accompanying file.

APPENDIX 11: PIMA SPECTRA AND LOGS FOR THE HERMIDALE AREA

See accompanying file.